Energy-quota-based integrated solutions for heating and cooling of residential buildings in the Hot Summer and Cold Winter zone in China

Article

Accepted Version

Published version at: http://dx.doi.org/10.1016/j.enbuild.2021.110767
To link to this article DOI: http://dx.doi.org/10.1016/j.enbuild.2021.110767

Publisher: Elsevier

Energy-quota-based integrated solutions for heating and cooling of residential buildings in the Hot Summer and Cold Winter zone in China

Xinyun Cao[a,b], Runming Yao[a,c*], Chao Ding[d], Nan Zhou[d*], Wei Yu[a,b], Jinyang Yao[e], Jie Xiong[a,b], Qiang Xu[f], Li Pan[f], Baizhan Li[a,b],

a Joint International Research Laboratory of Green Buildings and Built Environments (Ministry of Education), Chongqing University, Chongqing, 400045, China

b National Centre for International Research of Low-carbon and Green Buildings (Ministry of Science and Technology), Chongqing University, Chongqing, 400045, China

c School of the Built Environment, University of Reading, Reading, RG6 6DF, UK

d Lawrence Berkeley National Laboratory, Berkeley, CA 94720, USA

e University of British Columbia, BC, V6T 1Z4, Canada

f Shanghai Research Institute of Building Sciences Co., Ltd，Shanghai, 200032, China

*Corresponding authors: Joint International Research Laboratory of Green Buildings and Built Environments (Ministry of Education), Chongqing University, Chongqing 400045, China.

E-mail addresses: r.yao@reading.ac.uk (R. Yao)

*Corresponding authors: Lawrence Berkeley National Laboratory, Berkeley, CA, USA.

E-mail addresses: NZhou@lbl.gov (N. Zhou)

Abstract

The Hot Summer and Cold Winter (HSCW) climate zone along the Yangtze River Valley Region is an economically well-developed region in China. With the improvement of indoor thermal environments, the Chinese government implemented the control of energy use intensity (EUI) for heating and cooling to prevent the excessive growth of energy usage in the area. There is still a lack of EUI quota-based strategic and technical solutions for new residential buildings that consider both climate characteristics and residents' behaviour. This study set up a EUI quota-based three-step approach that consists of processes of multi-objective optimization, multi-criteria decision-making and integrated solutions analysis. The novel combined approach is implemented in this study that the NSGA-II solves the multi-objective optimization problem and TOPSIS solves the multi-criteria decision-making problem. By applying this novel approach, this study is the first to propose practical, integrated, cost-effective solutions for residential buildings while maintaining a comfortable indoor thermal environment that meets the EUI quota and can be implemented across the region. The proposed optimal integrated solutions are composed of both passive and active measures to improve building thermal performance, to reduce the burden on artificial heating and cooling while improving the performance of air conditioning in extreme weather conditions. This study mapped the full spectrum of solutions and provides rigorous evidence to energy policymakers for forthcoming design standards.

Keywords:

residential buildings, multi-objective optimization, decision-making, energy use intensity quota, Hot Summer and Cold Winter, life cycle cost

Acronyms

ACH	Air Change Rate per Hour $[h^{-1}]$
aPMV	adaptive Predicted Mean Vote
BEO	building energy optimization
CDD	Cooling Degree Days
COP	Coefficient of Performance for heating [W/W]
CRECS	China residential energy consumption survey
EER	Energy Efficiency Ratio for cooling [W/W]
EUI	Energy Use Intensity $[kWh \cdot m^{-2} \cdot a]$
GA	Genetic Algorithm
HP	mini-split ductless heat pump (HP)
HSCW	Hot Summer and Cold Winter climate zone
HVAC	Heating, ventilation, and air conditioning
HDD	Heating Degree Days
IC	sensitivity influence coefficient
LCC	Life Cycle Cost
MOST	the Ministry of Science and Technology of the People's Republic of China
NSGA-II	Non-dominated Sorting Genetic Algorithm II
PMV	Predicted Mean Vote
PSO	Particle Swarm Optimization

$SC_{Shading}$	shading coefficient of external shading device
SHGC	solar heat gain coefficient of the window
$SHGC_{com}$	Comprehensive Solar Heat Gain Coefficient of window and shading devices
TOPSIS	Technique for Order of Preference by Similarity to the Ideal Solution
WWR	Window-to-Wall Ratio
XPS	Extruded Polystyrene

1. Introduction

Excessive energy consumption can lead to increased carbon dioxide (CO_2) emissions, which are believed to adversely affect climate change [1]. As one of the largest energy consumers, China plays an important role in reducing CO_2 emissions and tackling climate change [2, 3]. At the Paris Conference on Climate Change 2015, China set a target for reducing its CO_2 emissions by 60%–65%, based on 2005 levels, by 2030 [4]. China's buildings (i.e., construction and operation) consumed 27.5% of the country's total energy consumption in 2001, and that increased to 36% in 2014 [5] due to its rapid urbanization. The residential sub-sector is the primary driver of growing energy demand in the building sector [6], accounting for more than 75% of newly built buildings [7]. Energy consumption for building heating and cooling is increasing due to continuing demand from the number of new buildings and changing thermal comfort expectations [8]. If we do not act on solutions, it will be impossible to achieve the carbon-reduction goal of reducing CO_2 emissions by 2030, which also could lead to a serious energy shortage [4]. The Chinese government has attached a great deal of importance to this situation and has released a series of energy efficiency policies in recent years [9-12] aimed at applying energy-efficient technologies to build ultra-low-energy buildings while maintaining a comfortable indoor environment and emphasizing energy-saving control in the entire process, including building design, construction and operation.

An effective way to achieve the national carbon-reduction target is to establish an energy quota system [13]. In 2016, the Chinese government proposed a total energy consumption quota system [14], implementing controls of both the amount of energy use and the energy use intensity (EUI). The energy quotas for different building types were proposed by Tsinghua University Building Energy Research Center based on the total amount of energy availability and the environmental capacity conditions of China in the future, combined with the energy demands from social and economic development [15]. For new residential buildings located in the Hot Summer and Cold Winter climate zone (HSCW), the quota of heating and cooling energy consumption for thermal comfort has been set at no more than 20 kilowatt-hours per square meter per annum ($kWh \cdot m^{-2} \cdot a$) [16]. In 2016, the Ministry of Science and Technology of the People's Republic of China (MOST) established a 13th Five Year Green Building

Flagship Programme (SSHCool project) aimed at achieving the EUI quota goal of limiting annual heating and cooling energy consumption to no more than 20 $kWh \cdot m^{-2} \cdot a$ in the Yangtze River Region within the HSCW climate zone[17].This was to be done by using integrated solutions composed of passive measures for building design and active measures to improve the performance of mechanical appliances. One of the most important goals of this programme was to provide a policy for instrumental measures and innovative technologies to demonstrate the achievability of the target EUI quota for heating and cooling.

1.1 Background information on the Hot Summer and Cold Winter climate zone

The majority of cities alongside the Yangtze River are categorized as part of the HSCW zone, which has a huge demand for cooling and heating [17]. The HSCW climate zone covers a wide, densely populated area with the fastest economic development [18], including 16 provinces, cities and autonomous regions. Since it is not as cold as the northern part of China, historically the HSCW zone, which is located south of the Huai River-Qin Mountain axis, is a non-central-heating area according to Chinese energy policy [19, 20]. In the absence of heating systems or appliances, the indoor thermal environment is severe. Li *et al*. [21] conducted a large-scale survey of indoor thermal environments and revealed that indoor air temperatures can reach to over 30℃ in summer and can be below 15℃ without any cooling/heating appliances in southern China. These temperatures are far beyond the comfort zone (18℃ to 26℃).

There is an increasing demand to improve indoor thermal environments due to economic growth, and this will no doubt increase heating and cooling energy consumption in the coming years. As evidence, the ownership of heating and cooling appliances per household is increasing year by year [22], and this will inevitably lead to a substantial increase in energy consumption. According to a recent large-scale survey, the mini-split ductless heat pump (HP) is the main appliance for heating and cooling in this region, since it offers zonal thermal comfort control, ease of maintenance and acceptable price [23]. As a stand-alone appliance, the operation mode, in terms of temperature setting and usage time, very much depends on residents' thermal comfort needs and behaviour [21]. The energy use mode has the characteristics of partial-space and intermittency, which relate to occupants' behaviour [24, 25]. Since the strategic and technical solutions for residential buildings are closely tied to residents' behaviour and climate conditions, they will be quite different from those of other regions.

The current compulsory implemented standards for residential buildings in the HSCW zone are summarized in Table 1. These standards are categorized into industry standards and local standards. The Design Standard for Energy Efficiency of Residential Buildings in Hot Summer and Cold Winter Zone (JGJ 134-2010), in bold in Table 1, is the only industry standard which covers the whole HSCW zone. The local standards of other cities or provinces were established based on this industry standard. However, the industry standard for residential buildings was released in 2010, and the thermal performance of a building's envelope could not meet the increased demands for both indoor thermal comfort and energy reduction. Ten years have passed since then, and because the economic level and residents' living habits have changed substantially, there is an urgent need to explore strategic and technical solutions for residential buildings to provide strong support for updating and formulating new standards.

Table 1: Summary of the current standards on residential buildings in the HSCW zone

No.	Name of standards	Code	Type	Release Time	Area
1	**Design standard for energy efficiency of residential buildings in the hot summer and cold winter zone**	**JGJ 134-2010**	**Industry-standard**	**2010**	**The whole HSCW zone**
2	Design standard for energy efficiency of residential buildings in Anhui province	DB 34/1466-2011	Local standards	2011	Anhui province
3	Design standard for residential buildings of low energy consumption in Hubei province	DB 42/T 559-2013	Local standards	2013	Hubei province
4	Design standard for energy efficiency of residential buildings in Sichuan province	DB 51/5027-2012	Local standards	2013	Sichuan province
5	Design standard for energy efficiency of residential buildings in Jiangxi province	DBJ/T 36-024-2014	Local standards	2014	Jiangxi province
6	Design standard of thermo-environment & energy conservation for residential buildings in Jiangsu province	DGJ 32/J 71-2014	Local standards	2015	Jiangsu province
7	Design standards on residential building energy-saving 65% (green building)	DBJ 50-071-2016	Local standards	2016	Chongqing
8	Design standard for energy efficiency of residential buildings in Shanghai	DGJ 08-205-2015	Local standards	2016	Shanghai
9	Design standard for energy efficiency of residential buildings in Hunan province	DBJ43/001-2017	Local standards	2017	Hunan province

1.2 Existing studies

The integrated solutions of passive building design measures and active measures were proposed as a solution for residential buildings in the HSCW zone [17]. Passive measures are available to minimize the energy consumption through natural means, and active measures aim to minimize the energy consumption of air-conditioning equipment in achieving comfortable conditions. This concept provides strategic guidance for solutions for residential buildings in this area. However, there is a need for more detailed, practical solutions and guidance, taking into account economic factors in the whole HSCW zone.

Research on passive technology for residential buildings in the HSCW zone has been extensive; for example, focusing on the optimal thickness of insulation materials for external walls [26, 27] and studying the adaptability of ventilation strategies [28, 29] and types of shading [30, 31]. It is obvious that the study on one single technology cannot support the revision of existing standards for residential buildings in the whole HSCW zone. When multiple technologies and multiple objectives exist, their optimization becomes a key issue for researchers. Table 2 summarizes some examples of existing studies focusing on multi-objective building energy optimization (BEO).

Table 2: Summary of the literature on building energy optimization (BEO)

Authors	Year	Location(s)	Building Types	Objective Functions	Design variables	Optimization algorithm	Energy use mode	Post-optimization process
Si *et al*. [32]	2019	Baltimore, Maryland	Office building	• Minimize the annual energy consumption.	• External wall insulation. • Building orientation. • Window upper positions in each façade. • Cooling design supply air temperature.	• Discrete Armijo gradient. • Hooke-Jeeves. • Particle swarm optimization with constriction coefficient. • Particle swarm optimization with inertia weight.	Continuous mode: full-time and full-space.	None
Li *et al*. [33]	2019	Hong Kong, China	Office building	• Minimize building energy demand. • Maximize the photovoltaic (PV) power generation.	• design variables of building envelope. • design variables of building energy system.	GA.	Continuous mode: full-time and full-space.	None
Ascione *et al.* [34]	2019	Italy	Residential building	• Minimize energy consumption. • Minimize global cost. • Minimize thermal discomfort.	• The setpoint temperatures. • The radiative properties of plasters. • The thermophysical properties of envelope components. • The window types. • The building orientation.	GA.	Continuous mode: full-time and full-space.	None
Gou *et al.* [35]	2018	Shanghai, China	Residential building	• Minimize discomfort time ratio. • Minimize building energy demand.	• Building orientation. • WWR at each façade. • Window U-value at each façade. • Window Solar Heat Gain Coefficient (SHGC) at each façade. • Window external shading at each façade. • Extruded polystyrene (XPS) board thickness. • External wall type at each façade.	NSGA-II.	Continuous mode: full-time and full-space.	None
Chen *et al*. [36]	2017	Hong Kong	Public rental housing	• Minimize energy consumption for heating and cooling. • Minimize energy consumption for lighting.	• Building orientation. • External wall. • External window. • Window-to-wall ratio (WWR). • Shading. • Infiltration.	NSGA-II.	Continuous mode: full-time and full-space.	None
Schwartz *et al.* [37]	2016	Sheffield, England	Residential building	• Minimize Life cycle cost. • Minimize Life cycle carbon footprint.	• Insulation materials. • Window types.	NSGA-II.	Continuous mode: full-time and full-space.	None
Asadi *et al*. [38]	2014	Coimbra, Portugal	School building	• Minimize energy use. • Minimize retrofit cost. • Minimize the total percentage of discomfort hours.	• External wall insulation materials. • Roof insulation materials. • Window types. • Solar collector types. • HVAC systems.	NSGA-II.	Continuous mode: full-time and full-space.	None

Bichiou *et al*. [39]	2011	Boulder, Chicago, Miami, Phoenix, San Francisco	Residential building	• Minimize LLC.	• External wall. • Roof. • External window. • WWR. • Infiltration. • Shading.	• GA. • PSO. • Sequential Search.	Continuous mode: full-time and full-space.	None

As shown in Table 2, many studies have focused on multi-objective BEO for various building types in different climates and countries considering various design variables. However, there are still research gaps. First, none of the previous studies focused on EUI quota. Second, in previous studies, boundary settings have assumed that the energy operation mode is “full-time full-space” (i.e., continuous operation for 24 hours daily for the whole apartment), which is not the actual situation in the HSCW zone where the “partial-time and partial-space” mode is more common. Third, in existing optimization studies, several studies worked out a set of best alternative solutions by applying an optimization algorithm; however, very few studies used the post-optimization process to find the single final optimal solution [40], which is a necessary process from a practical viewpoint. Since it is usually difficult to identify the best solution to meet every objective, there should be a trade-off decision-making process based on solutions to the Pareto-front solution set.

In summary, there is a lack of comprehensive strategic and technical solutions for residential buildings and a model that focuses on the target EUI quota while conducting the decision-making process and fully considering residents’ energy use behaviour.

1.3 Research objectives

To fill the knowledge gap, this study sought to work out cost-effective integrated solutions for residential buildings in the HSCW region to meet the EUI quota for heating and cooling while maintaining a comfortable indoor thermal environment. The principal of integrated solutions is to improve building thermal performance to extend the non-heating/cooling demand period, and to improve the performance of air conditioning to reduce the EUI of heating and cooling. A EUI quota-based integrated model that fully considers the climate characteristics and residents’ energy use behaviour in the HSCW zone was developed.

Comprehensive, systemic studies of integrated solutions to residential buildings based on the EUI quota have not been conducted previously. The originality and novelty of this study are demonstrated by the following features: (1) the combined multi-objective optimization process and multi-criteria decision-making process were innovatively developed in the methodology; (2) physical parameters, human thermal comfort demand, and lifecycle cost were included as an integral objective; (3) fully integrated localities of resident energy use behaviour were used; and (4) for the first time, the full spectrum of solutions were mapped to provide rigorous evidence to energy policymakers for forthcoming design standards.

2. Research methodology

2.1 Research framework

The non-dominated sorting genetic algorithm II (NSGA-II) method, which was proposed by Indian scholar

Deb [41], has been the most popular and effective algorithm for solving multi-objective problems in the study of BEO [36, 39, 42, 43]. NSGA-II is a type of genetic algorithm (GA) and has several advantages which can ensure the diversity of the population, avoid the loss of outstanding individuals and reduce the number of traditional GA calculations. Through applying NSGA-II, a set of points—called the Pareto-front solution set—can be reached, and these represent numerous best-alternative solutions. The multi-criteria decision-making method will help decision-makers evaluate these candidate solutions [44]. Among numerous methods, the technique for order of preference by similarity to the ideal solution (TOPSIS), one of the Euclidean distance-based decision-making methods, was most commonly used to deal with decision-making problems [45, 46]. TOPSIS calculates the Euclidean distance between each alternative solution and the positive ideal solution and ranks every alternative solution to identify the best one from the Pareto-front solution set [47]. Accordingly, NSGA-II can be the most effective optimization algorithm to obtain the Pareto-front solution set, and TOPSIS can help decision-makers successfully find the best solution from that set.

By combining NSGA-II and TOPSIS, a novel integrated BEO framework was developed, as shown in Figure 1. It contains three steps: (1) model setting for multi-objective BEO, (2) multi-criteria decision-making, and (3) optimal integrated solutions analysis. The purpose of the first step is to obtain the optimal Pareto-front solution set consisting of a set of passive solutions which meet the multiple objectives. The second step is a post-optimization process which aims to identify the best passive solution among the Pareto-front solution set by applying a multi-criteria decision-making method. The optimal integrated solution for residential buildings combining passive and active technologies can be worked out in the third step. Further explanations of each step follow:

1） Step 1: Model setting for multi-objective BEO

First, three objectives of this optimization model and the quantitative evaluation equations for multiple objectives are defined. Second, a basic building energy model is set up in EnergyPlus. Third, sensitivity analysis is performed on the typical model to identify the passive design variables with a significant impact on energy consumption. Then, the input values for the passive design variables are determined based on the results of the sensitivity analysis, to improve the optimization process efficiency. Fourth, the optimization model combining the EnergyPlus simulation program with the NSGA-II optimization algorithm is developed in Python. Finally, a set of optimal passive solutions, the Pareto-front set, is produced.

2） Step 2: Multi-criteria decision-making

The Pareto-front solution set consists of dozens or hundreds of passive solutions, it is difficult to directly determine one “best of the best” solution because of the complex and conflicting relationships between the design variables and objectives. Therefore, a multi-criteria decision-making method, TOPSIS, is applied to evaluate the different objectives to identify the best solution to be recommended as the passive technical solution for a typical city.

3） Step 3: Optimal integrated solutions analysis

This step analyzes the optimized integrated solution for each city that combines active and passive technologies and meets the requirements of the EUI quota, including the recommended thermal performance of external walls, roofs, external windows, shading types, infiltration rate, and recommended performance for heating and cooling.

The framework was implemented and demonstrated with a case study involving eight typical cities. Finally, the solutions for residential buildings in the HSCW zone were proposed to provide scientific support to policymakers to establish new regulatory guidance that will help achieve the targets of the EUI quota.

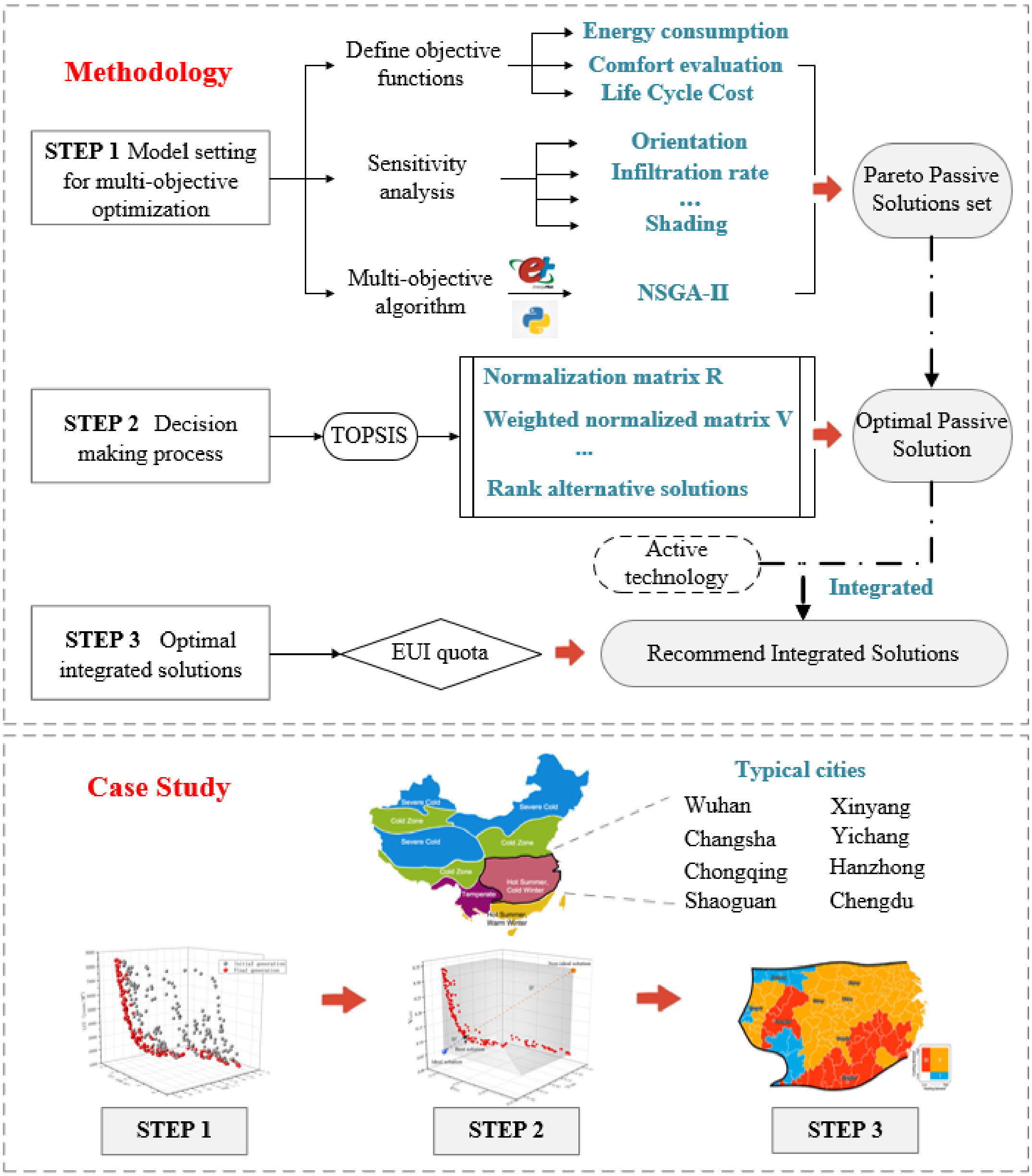

Figure 1: Framework for the energy-quota-based multi-objective BEO

2.2 Model setting for multi-objective BSO

2.2.1 Define objective functions

The optimization objectives of this study were to minimize annual energy use intensity (EUI) for heating and cooling, minimize the annual indoor thermal discomfort rate (TDR), and minimize the life cycle cost (LCC). The constraint equation of the three objectives can be described as follows:

$$\begin{cases} \text{Minimize } f1(x)=EUI \\ \text{Minimize } f2(x)=TDR \\ \text{Minimize } f3(x)=LCC \end{cases}$$

1) Energy use intensity (EUI) for heating and cooling

In this study, EUI was defined as the annual energy consumption for heating and cooling per building area, which can be calculated by EnergyPlus in each scenario. Since the HP is the main appliance for heating and cooling in the HSCW zone, the HP energy system model was set up in EnergyPlus.

2) Indoor thermal discomfort rate (TDR)

A quantitative measurement index was defined to evaluate the indoor thermal comfort condition. During the transition seasons, many buildings are not heated or cooled—this is called the “free-running” scenario. In the “free-running” scenario, the index of the adaptive predicted mean vote (aPMV) can be applied to evaluate the indoor thermal conditions, which was defined by the Chinese Evaluation Standard for Indoor Thermal Environments in Civil Buildings (GB/T 50785-2012) and considered behavioural adaptation [21, 48]. According to the standard GB/T 50785-2012, the value of aPMV varies from -0.5 to 0.5, with the highest thermal environment evaluation grade of 90% satisfactory. The value of aPMV each hour can be calculated by Equation (2.1), and if the value is beyond the comfort zone, the hour will be defined as a thermal discomfort hour. The thermal discomfort hours for the whole year will be measured for each solution. TDR is the ratio of thermal discomfort hours to total transitional hours, which reflects the indoor thermal discomfort condition during the transitional seasons. The smaller the TDR value, the better the indoor thermal comfort condition is.

The calculation method for aPMV was introduced in the Standard for the Evaluation of Indoor Thermal and Humidity Environments for Civil Buildings (GBT 50785-2012) [48]. It is shown in Equation 2.1:

$$aPMV = \frac{PMV}{1+\lambda \times PMV} \quad (2.1)$$

Equation (2.1) shows the relationship of the adaptive predicted mean vote (aPMV) and the predicted mean vote (PMV) in free-running buildings. The adaptive coefficient λ reflects a person’s adaptive functions, including both behavioural and psychological adaptation [49]. For residential buildings in the HSCW zone, the value of λ is 0.21

when PMV≥0, and the value of λ is -0.49 when PMV<0 [48].

3) Life cycle cost (LCC)

When comparing multiple technical solutions, it is often necessary to evaluate all the costs and benefits to obtain the life cycle cost (LCC) of the building. LCC is applied in the optimization model; it is the most widely used method to evaluate the cost-effectiveness of a building [44]. The building's total LCC is calculated using Equation 2.2 [39, 44, 50].

$$\mathrm{LCC} = C_{in} + C_o \quad (2.2)$$

In Equation 2.2, LCC refers to the net present value of the total life cycle cost, CNY/m^2. C_{in} refers to the net present value of the initial investment in building energy efficiency technologies, CNY/m^2. C_o refers to the net present value of the energy cost of HVAC devices during the operation period, CNY/m^2. Since this paper emphasizes the impact caused by changes in the thermal performance of design variables, the calculation of LCC is simplified by only considering the investment in the materials related to the thermal performance of the design variables.

1) The initial investment in building energy efficiency technologies, C_{in}

$$\mathrm{C}_{in} = \frac{C_{wall}+C_{win}+C_{roof}+C_{inf}+C_{sha}}{A} = \frac{(C_{i-wall}\cdot\delta_{wall}+C_{e-wall})\cdot A_{wall}+(C_{i-win}+C_{e-win})\cdot A_{win}+(C_{i-roof}\cdot\delta_{roof}+C_{e-roof})\cdot A_{roof}+C_{inf}+C_{sha}}{A} \quad (2.3)$$

Where C_{i-wall} and C_{i-roof} refer to the insulation material price of the external walls and roof respectively, in CNY/m^3; δ_{wall} and δ_{roof} refer to the thickness in millimetres (mm) of the insulation material of the external walls and roof, respectively; C_{i-win} refers to the price of glass, in CNY/m^2; and C_{e-wall}, C_{e-win} and C_{e-roof} refer to the installation labour costs of the insulation materials for the external walls, external windows, and roof, respectively, in CNY/m^2. A_{wall}, A_{win} and A_{roof} refer to the areas in square meters of the external wall, windows, and roof respectively; A refers to the total building area, in square meters. The prices of construction materials and labour costs in different cities and different companies fluctuate greatly. This study intensively investigated popularly used domestic materials and the manufacturers' product categories and obtained the average market price with taxes. For example, the price of extruded polystyrene (XPS), the most commonly used insulation material for external walls and roofs, is 712.77CNY/m^3. The price of double-layer glass is 116.51 CNY/m^2. The price of triple-layer glass is 266.00 CNY/m^2. The price of double-layer low emissivity (Low-E) glass is 163.39 CNY/m^2. The installation labour cost is 30 CNY/m^2.

2) Energy cost of heating and cooling during the operation period, C_o

Considering the time value of the cost, the future recurrent expenses are converted to present costs. Assuming that the annual energy consumption is the same, the calculation equation for the energy cost of HVAC devices during an operation period is as follows [50]:

$$C_o = E \cdot C_e[1-(1+I)^{-N}]/I \quad (2.4)$$

Where E refers to simulated annual energy consumption for heating and cooling, $kWh/m^2 \cdot a$. C_e refers to the local electricity price in CNY/kWh. The average price of electricity for residential buildings in hot summer and cold winter areas is 0.53 CNY/kWh. N refers to operation period, and the value of N is 20 [51]. I refers to the bank interest rate as a percentage. At the time of writing, the interest rate is 4.9% according to the Bank of China website.

2.2.2 Sensitivity study

Since energy is the most important factor considered in this study, the sensitivity of various factors to energy demand was analyzed. The purpose of the sensitivity analysis can be described as follows: (1) to identify the main factors affecting energy demand and provide technical support for the decision-making process and (2) to filter out some unimportant variables and narrow the range of input variables for the optimization model, and to reduce the operation time of the optimization process.

The sensitivity analysis methods can be divided into local sensitivity analysis and global sensitivity analysis [35]. Compared with the global sensitivity analysis, the local sensitivity analysis has the advantage of requiring less computer time. A local sensitivity analysis is also called the "one-factor-at-a-time" method, which changes one of the factors during the analysis while the values of other factors are fixed. Local sensitivity analysis is based on the assumption that the model is expressed as $y = f(x_1, x_2, \dots, x_n)$ ($x_i$is the ith variable value of the model), each variable changes within the range of possible values to predict how the output value changes according to changes in the input value. The impact of the output value is called the sensitivity influence coefficient (IC) of the variable. The larger the IC value, the greater the influence of the variable on the output of the model. The rank of the IC for each variable can be used to identify the factor that plays a leading role in building energy consumption. IC can be calculated by Equation 2.5 [52]. There are 14 variables for sensitivity analysis in this study. The range of input variables is shown in Table 3.

$$\mathrm{IC} = \frac{change\ in\ output}{change\ in\ input} = \frac{\partial OP}{\partial IP} \approx \frac{OP-OP_{bc}}{OP_{bc}} \div \frac{IP-IP_{bc}}{IP_{bc}} \quad (2.5)$$

The range of orientation varies from -15° to 15° according to the range recommended by the Chinese residential design standards of Hunan province (DBJ43/001-2017), Hubei province (DB 42/T 559-2013), Jiangxi province (DBJ/T 36-024-2014), and Anhui province (DB 34/1466-2011). The base value for orientation is 0, which means south-north.

The minimum requirement of fresh air for residential buildings according to the Design Code for the Heating Ventilation and Air Conditioning of Civil Buildings (GB50736-2012) standard is 0.5 times per hour; while the base-case value of the infiltration rate is 1.0 times per hour according to the compulsory Energy-saving Design Standards for Residential Buildings in Hot Summer and Cold Winter Zone (JGJ134-2010) standard. Therefore, the candidate input values for the infiltration rate are $0.5h^{-1}$ and $1.0h^{-1}$.

The typical structures of external walls and roofs for residential buildings in this area are shown in Table 4 and Table 5. As the thickness of the insulation material named XPS increases from 20 mm to 100 mm, the U-value of an external wall and roof decreases gradually. The candidate input U-values for external walls range from 0.26 $Wm^{-2}K^{-1}$ to 0.83 $Wm^{-2}K^{-1}$, while the candidate input U-values for a roof range from 0.27 $Wm^{-2}K^{-1}$ to 0.72 $Wm^{-2}K^{-1}$.

The range of the U-value and SHGC for external windows is determined by the normal range of glasses. The range of the window-to-wall ratio (WWR) in Table 3 is defined by a consideration of the reasonable size of a window and the limits of the requirements specified in the aforementioned standard JGJ 134-2010. Venetian blinds are recommended in residential buildings across this area [53], therefore external vertical Venetian blinds are applied in this model, and the blinds are assumed to cover the whole window when the solar radiation intensity is greater than 100 Wm^{-2} from May to September [53]. $SC_{Shading}$ refers to the shading coefficient of the external shading; it is the main thermal performance of external shading devices. The value of $SC_{Shading}$ is 0.4 when the blinds completely cover the window (calculated according to the standard [53]). In the scenario without any shading devices, the value of $SC_{Shading}$ is 1.0. Two shading scenarios are considered in this study: one is no shading, and the other is the application of venetian blinds, hence the candidate input values of $SC_{Shading}$ are 1.0 and 0.4.

Table 3: Input variables and their ranges for sensitivity analysis

No.	Variables	Description	Base value	Probability	Range
X1	Orientation	Degrees from true North [°]	0	Continuous Uniform	[-15, 15]
X2	Infiltration Rate	ACH [h^{-1}]	1.0	Discrete	(0.5,1.0)
X3	External Wall	U-value [$Wm^{-2}K^{-1}$]	0.83	Discrete	(0.26, 0.28, 0.31, 0.35, 0.39, 0.45, 0.53, 0.65, 0.83)
X4	Roof	U-value [$Wm^{-2}K^{-1}$]	0.72	Discrete	(0.27, 0.29, 0.33, 0.37, 0.42, 0.48, 0.58, 0.72)
X5	External Window	U-value [$Wm^{-2}K^{-1}$]	2.8	Continuous Uniform	[1.0, 2.8]
X6		SHGC	0.9	Continuous Uniform	[0.3, 0.9]
X7	WWR - East (E)	--	0.15	Continuous Uniform	[0.15, 0.20]
X8	WWR - West (W)	--	0.15	Continuous Uniform	[0.15, 0.20]
X9	WWR - South (S)	--	0.30	Continuous Uniform	[0.30, 0.50]

X10	WWR - North (N)	--	0.20	Continuous Uniform	[0.20, 0.40]
X11	Shading - East (E)	$SC_{Shading}$	1.00	Discrete	(0.4, 1.0)
X12	Shading - West (W)	$SC_{Shading}$	1.00	Discrete	(0.4, 1.0)
X13	Shading - South (S)	$SC_{Shading}$	1.00	Discrete	(0.4, 1.0)
X14	Shading - North (N)	$SC_{Shading}$	1.00	Discrete	(0.4, 1.0)

Table 4: Structures of typical external wall

No.	**Cement mortar [mm]**	**XPS [mm]**	**Cement mortar [mm]**	**Sintered shale porous brick masonry [mm]**	**Cement mortar [mm]**	**U-value $[Wm^{-2}K^{-1}]$**
1 (Base)	**5**	***20***	**20**	**200**	**20**	***0.83***
2	5	*30*	20	200	20	*0.65*
3	5	*40*	20	200	20	*0.53*
4	5	*50*	20	200	20	*0.45*
5	5	*60*	20	200	20	*0.39*
6	5	*70*	20	200	20	*0.35*
7	5	*80*	20	200	20	*0.31*
8	5	*90*	20	200	20	*0.28*
9	5	*100*	20	200	20	*0.26*

Table 5: Structures of typical roof

No.	**Crushed stone [mm]**	**Cement mortar [mm]**	**XPS [mm]**	**SBS modified bitumen waterproofing membrane [mm]**	**Cement mortar [mm]**	**All-light concrete （1,051～1,150） [mm]**	**Reinforced Concrete [mm]**	**U-value $[Wm^{-2}K^{-1}]$**
1 (Base)	**20**	**20**	***30***	**5**	**20**	**30**	**120**	***0.72***
2	20	20	*40*	5	20	30	120	*0.58*
3	20	20	*50*	5	20	30	120	*0.48*
4	20	20	*60*	5	20	30	120	*0.42*
5	20	20	*70*	5	20	30	120	*0.37*
6	20	20	*80*	5	20	30	120	*0.33*
7	20	20	*90*	5	20	30	120	*0.29*
8	20	20	*100*	5	20	30	120	*0.27*

2.2.3 Multi-objective BSO model combining NSGA-II and EnergyPlus

The application of multi-objective optimization methods have been extensively applied in the field of building energy efficiency. Genetic algorithms (GA), Particle Swarm, and Sequential Search are the three main multi-objective optimization algorithms. GA was the most accepted and applied algorithm to solve multi-objective problems[54]. Farshad Kheiri[55] pointed out that since 2000, the application rate of GA has increased rapidly, which is much higher than other methods. Indian scholar Deb[56] improved GA and proposed the NSGA-II method. Compared with the traditional GA method, NSGA-II has several advantages which can ensure the diversity of the population, avoid the loss of outstanding individuals, and reduce the number of traditional GA calculations. GA has been used in building and HVAC system optimization research in the past decade, and NSGA-II can solve the multi-objective optimization problem of building design very effectively[39, 42, 43]. The combined approach perfectly solve the problem in dictated in this study.

Based on previous analyses, a multi-objective optimization model combining an optimization algorithm (NSGA-II) with a simulation program (EnergyPlus) was set up. This model runs on the Python platform. There are 14 input variables, as shown in Table 3. The detailed logic of the optimization model is illustrated in Figure 2 and explained in the following steps [37]：

(i) Generate the initial geometry of the model in the SketchUp platform and export an IDF file to EnergyPlus.

(ii) Determine the range for the 14 input variables (Table 3) and set the values of the NSGA-II algorithm. The parameters of the optimization algorithm are set as follows: population size = 50, number of generations = 30, crossover probability = 0.9, and mutation probability = 0.355 [43].

(iii) The model randomly assigns values of input variables within possible ranges to generate an initial population. Every individual in the population represents a solution. EnergyPlus obtains input data and generates an EnergyPlus model file for every individual, then the model is simulated and the results read by Python to calculate the fitness function values of each individual in the whole population. The fitness function values in this study are EUI, LCC and TDR.

(iv) The fitness function value of each individual is fed back to the NSGA-II algorithm. The algorithm performs the genetic operations of selection, mutation and crossover to select individuals for evolution. Non-dominated sorting, distance calculation of crowdedness, and elite reservation are also conducted to generate the next generation of the population.

(v) The loop calculation is run until the set termination algebra is reached.

(vi) All individuals in the last generation of the population form the Pareto-front solution set. In this study, the Pareto-front solution set was a set of passive technical solutions.

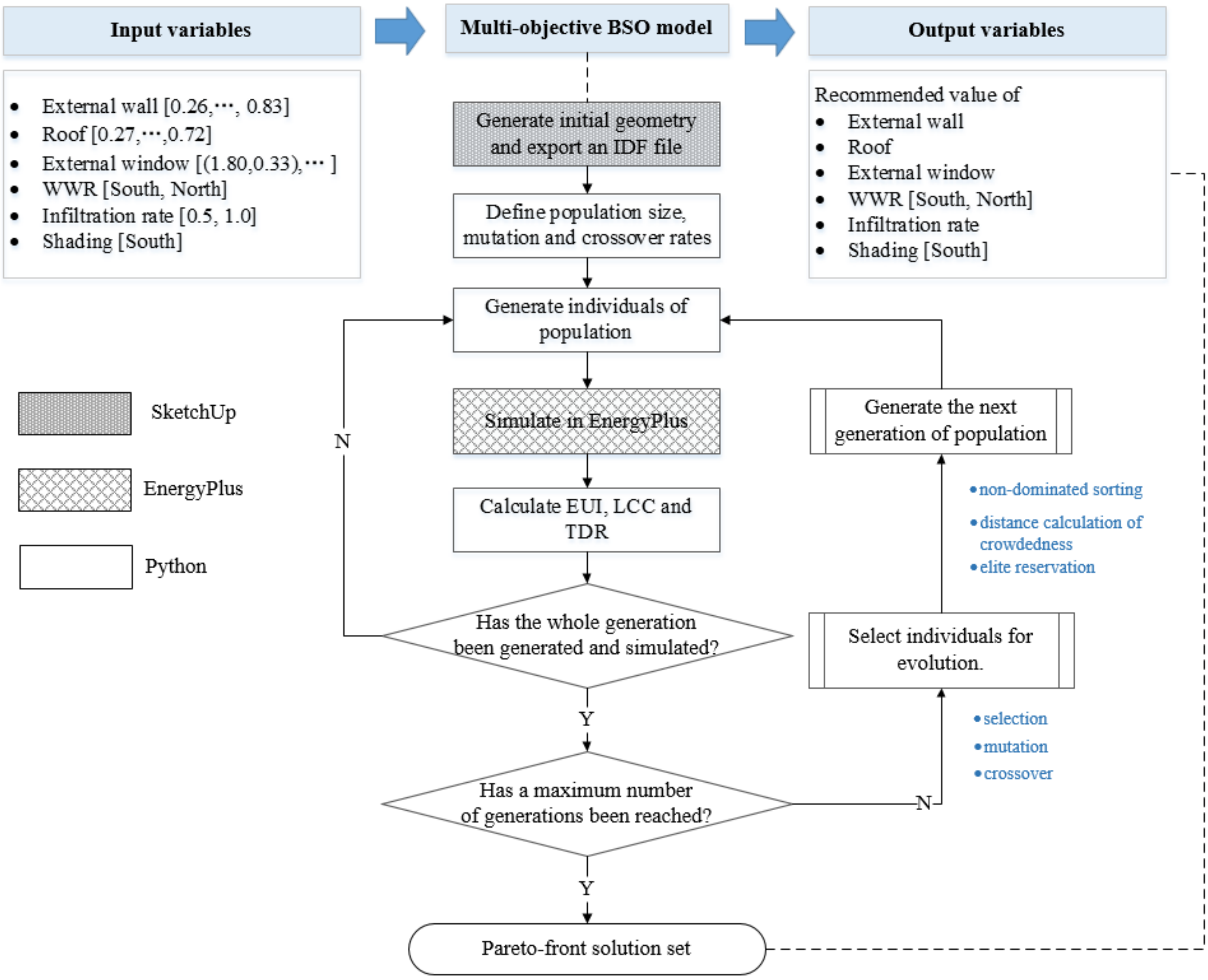

Figure 2: Logic of the multi-objective BSO model

2.3 Multi-criteria decision-making

Through the multi-objective optimization model, a Pareto-front solution set that meets the three objectives of each typical city can be obtained, but the problem has not been completely solved so far. The optimal solution must then be identified among the Pareto-front solution set. A multi-criteria decision-making method is used to solve this problem. The TOPSIS decision-making method is the Euclidean distance-based method that identifies the optimal solution by calculating the relative distance of the alternative solutions from the ideal solution. For n-dimensional criteria, the TOPSIS method calculation steps are as follows [57-59]:

(i) Setting up a multiple-criteria decision-making matrix D

A decision-making matrix *D* with *n* criteria and *m* alternative solutions is set up according to the Pareto-front solution set. Each criterion value for each solution can be expressed as x_{ij}:

$$D = \begin{pmatrix} & C_1 & C_2 & \dots & C_n \\ A_1 & x_{11} & x_{12} & \dots & x_{1n} \\ A_2 & x_{21} & x_{22} & \dots & x_{2n} \\ \dots & \dots & \dots & \dots & \dots \\ A_m & x_{m1} & x_{m2} & \dots & x_{mn} \end{pmatrix}$$

where $A_1, A_2, \dots, A_m$ are alternative solutions and $C_1, C_2, \dots, C_n$ are criteria.

(ii) Setting up normalization matrix *R*

Normalize the matrix by applying Equation 2.6.

$$r_{ij} = \frac{x_{ij}}{\sqrt{\sum_{i=1}^{m} {x_{ij}}^2}}, i = 1,2, \dots, m \; and \; j = 1,2, \dots, n \quad (2.6)$$

The normalized decision matrix is $R = [r_{ij}]_{m \times n}$。

(iii) Calculating the weighted normalized matrix *V*

$$V = [v_{ij}]_{m \times n}, \text{ where } v_{ij} = w_j \cdot r_{ij}, i = 1,2, \dots, m \text{ and } j = 1,2, \dots, n, \quad (2.7)$$

where w_j refers to the weight of the j-th criteria, and $\sum_{j=1}^{n} w_j = 1$.

In this study, three objectives need to be weighed, and the importance of each of the three objectives is defined by the corresponding weight. The weights of EUI, TDR and LLC are 0.33, 0.33 and 0.33, respectively.

(iv) Positive Ideal Solution D^+ and Negative Ideal Solution D^-

For a maximization problem like benefit criteria, the positive ideal solution D^+ is the combination of the maximum values in each criterion column in the matrix. The negative ideal solution D^- is the combination of the minimum values in each criterion column in the matrix. Conversely, for a minimization problem like cost criteria, the positive ideal solution D^+ is the combination of the minimum values in each of the criterion columns. The negative ideal solution D^- is the combination of the maximum values in each criterion column in the matrix.

$$D^+ = \{{v_1}^+, {v_2}^+, \dots, {v_n}^+\}, \quad (2.8)$$

$$D^- = \{{v_1}^-, {v_2}^-, \dots, {v_n}^-\}, \quad (2.9)$$

where $${v_j}^+ = \{(\max v_{ij} \,|j \in J_1), (\min v_{ij} \,|j \in J_2) | i = 1,2, \dots, m\}$$

$${v_j}^- = \{(\min v_{ij} \,|j \in J_1), (\max v_{ij} \,|j \in J_2) | i = 1,2, \dots, m\}$$

J_1 refers to the maximization problem criteria, and J_2 refers to the minimization problem criteria. In this study, three objectives belong to J_2.

(v) N-dimensional Euclidean Distance

The n-dimensional Euclidean distance from the alternative solutions to the positive ideal solution D^+ and negative ideal solution D^- can be calculated as follows:

$$D^+ = \sqrt{\sum_{j=1}^{n} (v_{ij} - {v_j}^+)^2}, i = 1,2, \dots, m \quad (2.10)$$

$$D^{-}=\sqrt{\sum_{j=1}^{n}\left(v_{ij}-v_{j}^{-}\right)^{2}}, i=1,2,\ldots,m \quad (2.11)$$

(vi) Relative closeness to the ideal solution

The relative closeness, C^*, to the ideal solution can be calculated by applying Equation 2.12. The larger the value of C^*, the closer the alternative solution to the positive ideal solution, D^+.

$$C^{*}=\frac{d_i^{-}}{d_i^{+}+d_i^{-}}, i=1,2,\ldots,m \quad (2.12)$$

(vii) Rank alternative solutions

For rank alternative solutions according to the calculated C^*, the larger the value of C^*, the better the performance of the alternative solution. The solution with the largest value of C^* from the Pareto-front solution, the set is the best one.

2.4 Optimal integrated solutions combining passive and active technologies

According to the EUI quota for residential buildings in the HSCW zone, Yao *et al*. [17] proposed the integrated optimal solutions combining passive technologies for building design and active measures with improved equipment performance to extend the non-heating and cooling period and to reduce the heating and cooling energy consumption. First, proper application of passive technologies—such as the improved thermal performance of the building envelope, the use of proper shading devices and a ventilation strategy—can reduce the heating/cooling load to extend non-heating and non-cooling time, all while reducing the peak load and flattening the peak curve. Second, energy efficiency equipment with higher performance will be produced through innovative engineering solutions when active measures (artificial heating/cooling) are inevitably used for the extreme climates in summer and winter. It is believed neither solution on its own can meet both the EUI quota requirements and the thermal comfort targets for this region. Based on the concept of an integrated solution, this paper sought to work out the optimal integrated solutions for residential buildings in typical cites in the HSCW zone.

2.5 Case study

2.5.1 Climate analysis in typical cities

Xiong *et al*. [60] proposed seven sub-climatic zones within the HSCW zone, using the method of cluster analysis based on the meteorological data from 166 meteorological stations over the last 10 years. Based on the sub-climate zones and geographic location, eight cities with different heating and cooling demand were selected as typical cities (Figure 3).

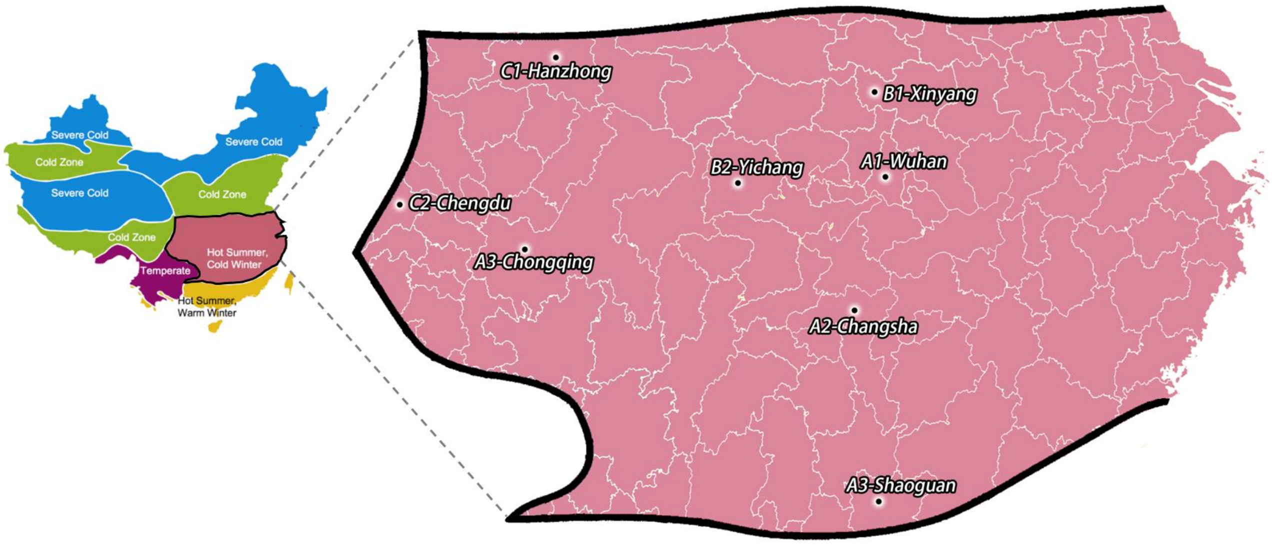

Figure 3: Location of typical cities in the HSCW zone

Figure 4 and Table 6 illustrate the climate characteristics of each selected city. As seen in Figure 4, the values in the blue box represent the outdoor dry bulb temperature in the coldest month (January), which can be as low as -8℃ in Xinyang. The values in the orange box represent the average outdoor dry bulb temperature in the hottest month (July), which can be as high as 40℃ in Wuhan.

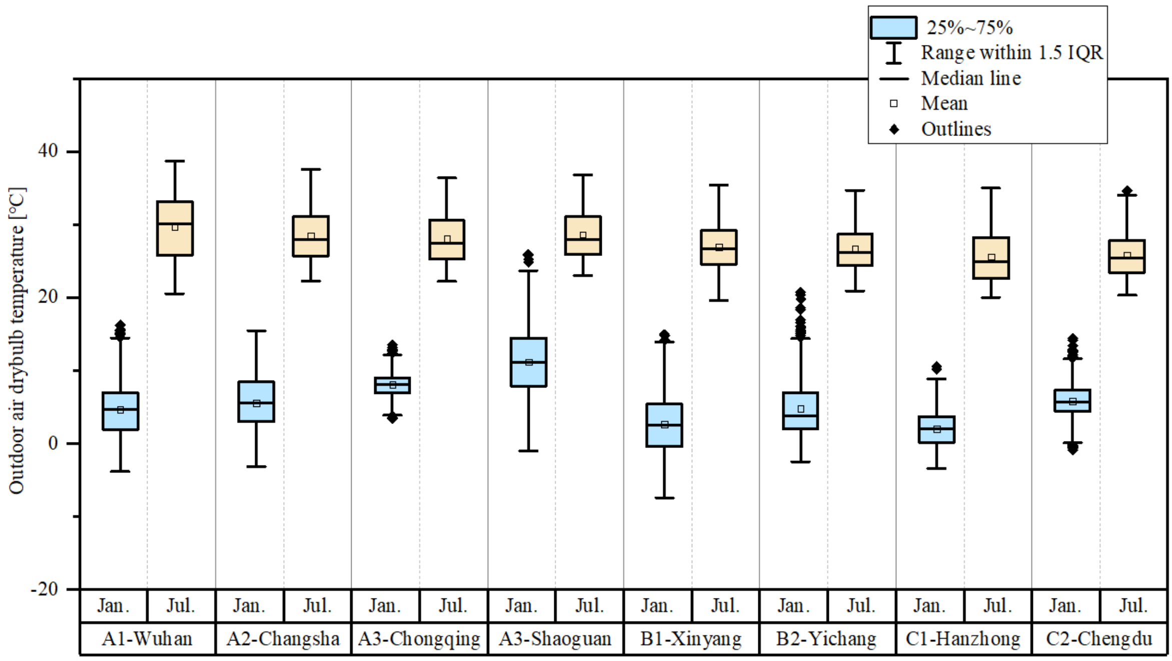

Figure 4: A comparison of the characteristics of typical cities [Data source: EnergyPlus weather file]

The heating and cooling demands for each city are categorized into three levels: high, medium and low [60]. Wuhan has the highest demand for both heating and cooling, while Chengdu has the lowest heating demand and medium cooling demand. More detailed information for each city can be found in Table 6. Based on the heating and cooling demands, the eight cities were divided into three areas. Cities with low cooling demand were classified as Area I, relatively heating-dominated cities. Cities with low heating demand were classified as Area III, relatively cooling-dominated cities. Cities with both medium or high heating/cooling demand were classified as Area II.

Table 6: Climate characteristics of typical cities

Area	Province	City	Climatic description [60]			HDD base 18 ℃ [61]	CDD base 26 ℃ [61]
			Sub-climatic zones	Cooling demand	Heating demand		
I	Shaanxi	Hanzhong	C1	Low	High	1945	63
	Sichuan	Chengdu	C2	Low	Medium	1344	56
II	Hubei	Wuhan	A1	High	High	1501	283
	Hunan	Changsha	A2	High	Medium	1466	230
	Henan	Xinyang	B1	Medium	High	1863	137
	Hubei	Yichang	B2	Medium	Medium	1437	159
III	Chongqing	Chongqing	A3	High	Low	1089	217
	Guangdong	Shaoguan	A3	High	Low	747	249

HDD = heating degree days; CDD = cooling degree days

2.5.2 Base building model setting

There are two main residential building forms in HSCW zone, the slab-type and the point-type. Slab-type residential building is more common in HSCW zone [62], therefore a slab-type building is selected as the reference building in this study. The slab-type building with a rectangular footprint has the advantages of better natural ventilation and natural light conditions [35].By reviewing over 70 architectural design plans of newly built residential buildings in the region, a reference building floor layout was determined, as shown in Figure 5.

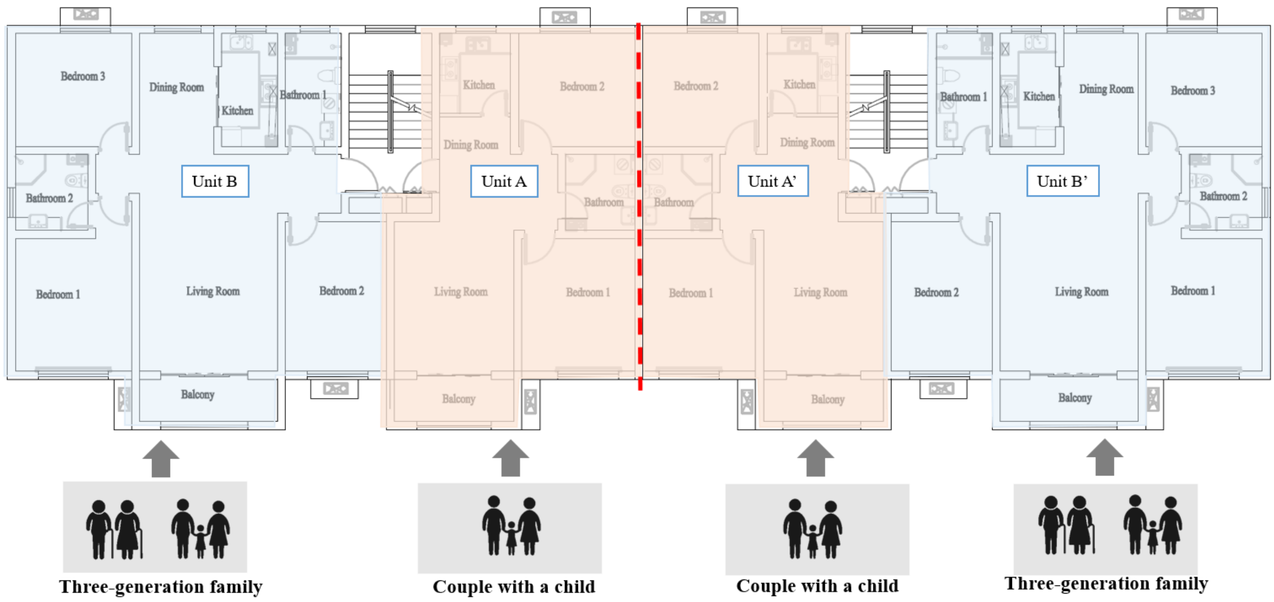

Figure 5: The layout of the standard floor of the reference building

The standard floor consists of four units. There are two bedrooms and one bathroom in Unit A and A', with a building area of 70 ㎡ each. As shown in Figure 5, a family consisting of a working couple and a school-aged child are supposed to live in this kind of unit. There are three bedrooms and two bathrooms in Unit B and B', with a building area of 108 ㎡ each. A family of six people, with three generations, are supposed to live in this kind of unit. According to the results of a large-scale survey by Chongqing University in five main cities in the HSCW zone, the occupancy pattern for two kinds of families can be seen in Table 7 [23].

Table 7: Occupancy pattern

Unit type	**Family structures**	**Space**	**Time**					
			00:00-7:00	8:00-12:00	13:00-14:00	15:00-18:00	19:00-22:00	23:00-24:00
Type A	Couple with a child	Living room	×	×	×	×	√	×
		Bedroom	√	×	×	×	×	√
Type B	Three-generation family	Living room	×	√	×	√	√	×
		Bedroom	√	×	√	×	×	√

√ refers to occupied, × refers to unoccupied.

Energy consumption for heating and cooling were simulated by EnergyPlus. The input information of the base building model in EnergyPlus can be seen in Table 8.

Table 8: Main base input information of a reference building in EnergyPlus

Parameter	**Input set description**	**References**
Building orientation	South-north direction	[63]
HVAC	The mini-split ductless heat pump (HP)	[23]
Heating setpoint	18℃	[63]
Cooling setpoint	26℃	
Cooling EER / heating COP	2.69/2.10 [W/W] 1) Heat pump air conditioner units (secondary energy efficiency). 2) Considering the actual operating effect is 80% of the rated operating conditions.	[64]
Human heat dissipation	116.30 Wm^{-2}（Standing scenario, moderate labour r ）	[48]
	69.78 Wm^{-2}（Sitting scenario）	
Equipment power	4.3 Wm^{-2}	[63]
Lighting power	6 Wm^{-2}	[63]
Ventilation strategy	If the outdoor weather conditions are suitable for ventilation (when the outdoor temperature is 18℃ to 26℃), the windows will be open for natural ventilation. The natural ventilation rate changes according to indoor and outdoor heat pressure and wind pressure.	[63]
Shading type	The shading form of the base model is Venetian blind. When the solar radiation intensity is greater than 100 Wm^{-2} (from May to September), the Venetian blinds completely cover the whole window.	[53]
Air infiltration rate	$1(h^{-1})$	[63]

EER = energy efficiency ratio for cooling; COP = coefficient of performance for heating

Table 9 shows two different types of heating and cooling schedules. The current heating and cooling schedule was proposed by Chao et al. [65] according to China Residential Energy Consumption Survey (CRECS) data conducted by Renming University in 2012 [66]. The survey data includes 1,450 residential buildings across 26 provinces, and 218 valid instances from the HSCW zone were selected to calibrate the base case model in this paper [65]. The residents tend to use the HP only when the weather is too hot or too cold, to save on electricity bills, but sacrifice thermal comfort. To meet the increasing occupants' thermal comfort demands, ideal heating and cooling schedule are assumed in this paper (Table 9). The ideal HVAC devices can maintain indoor air temperature within the comfortable range during occupied hours, the occupied schedule is an intermittent and partial-space mode and is described in Table 7.

Table 9: Heating and cooling schedule

	Heating and cooling schedules	**References**
Current schedule	Heating Schedule: 19:00–22:00, January 1 to February 14 Cooling Schedule: 18:00–22:00, July 18 to August 31	[65]
Ideal schedule	Cooling period: June 15 to August 31 Heating period: December 1 to February 28 (the next year)	[23]
	Intermittent and partial-space operation mode: maintaining the indoor air temperature within the comfortable range (18℃ to 26℃) during the occupied time (occupied schedule can be found in Table 7).	Assigned in this paper

3. Results

3.1 Calibration of the base case model

As illustrated in Section 2.5.1, Wuhan is located in the middle of the HSCW zone and has the highest demand for both cooling and heating. Wuhan was selected as a typical city to calibrate the base case simulation model with actual building energy survey data. The heating and cooling schedule was set as the current schedule shown in Table 9, and the current heating/cooling energy consumption and total building electricity consumption were simulated using EnergyPlus. As shown in Figure 6, the simulated heating and cooling energy consumptions account for 32% of the total building electricity consumption, which is consistent with the results of other scholars [65]. The simulated current annual heating and cooling EUI was 8.32 $kWh \cdot m^{-2}$ (Figure 6), and it matched well with the research conducted by Tsinghua University. The research revealed that the current annual heating and cooling EUI of residential buildings in the HSCW zone is about 8 $kWh \cdot m^{-2} \cdot a$, with residents sacrificing thermal comfort [67]. The simulated total building electricity consumption was 25.54 $kWh \cdot m^{-2}$ (Figure 6), and it is consistent with the average residential building electricity consumption which was 25.8 $kWh \cdot m^{-2}$ (Figure 7) according to the CRECS survey [65]. Therefore, the model can be considered well calibrated.

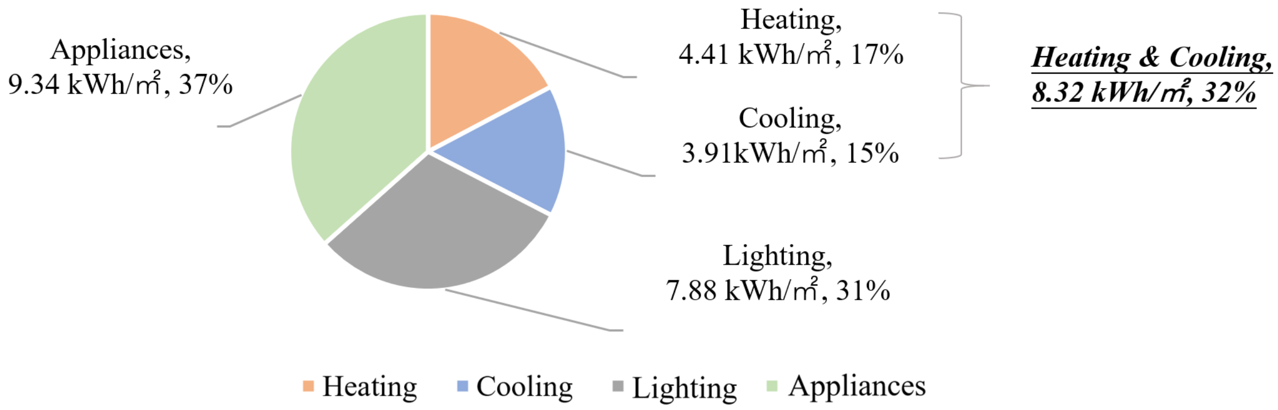

Figure 6: Base case residential building simulated energy consumption breakdown

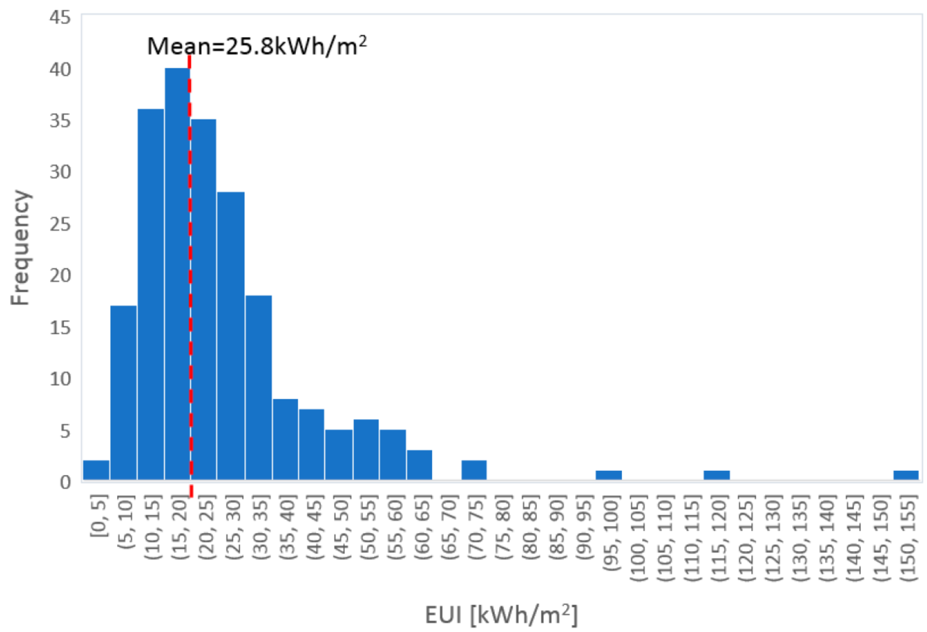

Figure 7: Distribution of electricity consumption (CRECS survey) [65]

3.2 Ideal EUI of the base case model

To improve residents' indoor thermal comfort, this study assumed an ideal heating and cooling schedule (Table 9). The annual EUI for both cooling and heating of the base building in different cities is shown in Figure 8. The values of the envelope all meet the requirements of the current residential energy-saving standards; see Section 2.5.2 for more detailed information on the base case scenario. To maintain indoor comfort, the total annual EUI for cooling and heating in the base case scenario is between 26.4 ~ 39.4 $kWh \cdot m^{-2}$, which is far from the target quota of 20 $kWh \cdot m^{-2}$. The total annual EUI for heating and cooling varies considerably among these cities, with Wuhan having the highest total energy consumption and Chengdu having the lowest. The top two cities with the lowest cooling energy consumption are Hanzhong and Chengdu, and the top two cities with the lowest heating energy consumption are Shaoguan and Chongqing. The energy consumption for heating and cooling in the remaining four cities are both relatively high.

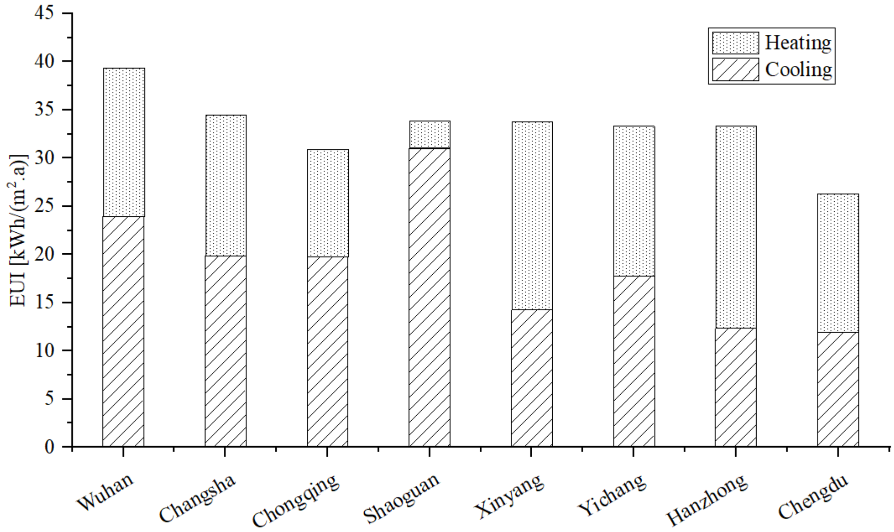

Figure 8: EUI of the base-case model in typical cities

3.3 Sensitivity analysis study

The main purpose of the sensitivity analysis is to identify the impact of various passive factors on building energy consumption, thereby reducing the input variables, which will greatly reduce the operation time of the BSO model. All the sensitivity influence coefficients (IC) of the parameters for annual total heating and cooling load were calculated (Figure 9). The ranking trend of sensitivity coefficients for all parameters was consistent in most typical cities. The ICs for the top seven parameters are listed in Table 10. The conclusions are summarized as follows:

(i) To reduce the cooling load, the top seven parameters are external window - SHGC (X6), window-to-wall ratio - S (X9), infiltration rate (X2), shading type - S (X13), window-to-wall ratio - N (X10), shading type - N (X14), and external windows - U value (X5).

(ii) To reduce the heating load, the top seven parameters are infiltration rate (X2), external wall - U value (X3), external windows - SHGC (X6), external windows - U value (X5), roof - U value (X4), window-to-wall ratio - S (X9), and window-to-wall ratio - W (X8).

(iii) To reduce the total annual heating and cooling load, the top seven parameters are infiltration rate (X2), external walls - U value (X3), external windows - SHGC (X6), shading type - S (X13), window-to-wall ratio - S (X9), window-to-wall ratio - N (X10), and roof - U value (X4).

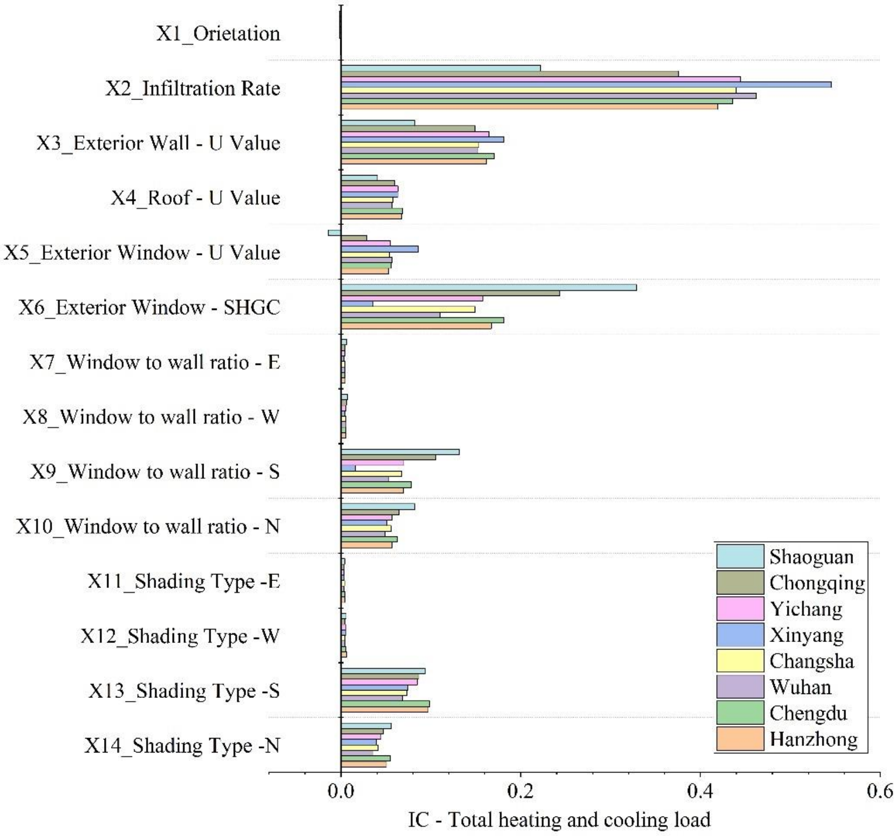

Figure 9: Sensitivity analysis of passive design parameters for annual total heating and cooling load

Table 10: Sensitivity ranking for the top seven parameters

Rank	Cooling load $[kWh \cdot m^{-2} \cdot a]$	Heating load $[kWh \cdot m^{-2} \cdot a)]$	Total annual heating and cooling load $[kWh \cdot m^{-2} \cdot a]$
1	X6_External Windows - SHGC	X2_Infiltration Rate	**X2_Infiltration Rate**
2	X9_Window-to-wall ratio - S	X3_External Wall - U-value	**X3_External Wall - U-value**
3	X2_Infiltration Rate	X6_External Windows - SHGC	**X6_External Windows - SHGC**
4	X13_Shading Type - S	X5_External Windows - U-value	**X13_Shading Type - S**
5	X10_Window-to-wall ratio - N	X4_Roof - U-value	**X9_Window-to-wall ratio - S**
6	X14_Shading Type - N	X9_Window-to-wall ratio - S	**X10_Window-to-wall ratio - N**
7	X5_External Window - U-value	X8_Window-to-wall ratio - W	**X4_Roof - U-value**

Based on the sensitivity ranking, the top seven parameters in bold font in Table 11 were selected as input variables for the optimization model. The other seven parameters have a low impact on energy consumption and remain constant (base-case values). Besides, three real typical window types were selected in the optimization process: double-layer glass, triple-layer glass and double-layer Low-E glass. Table 12 shows the structures of each window type.

Table 11: Selection of the influential variables

Variables	Categories	Description of variables	Probability	Base-case values	Sampling ranges
X1	Orientation	Building long axis azimuth [°]	--	0	0 (constant)
X2	**Infiltration Rate**	**ACH [h^{-1}]**	**Discrete**	**1.0**	**(0.5, 1.0)**
X3	**External Wall**	**U-value [$Wm^{-2}K^{-1}$]**	**Discrete**	**0.83**	**(0.26, 0.28, 0.31, 0.35, 0.39, 0.45, 0.53, 0.65, 0.83)**
X4	**Roof**	**U-value [$Wm^{-2}K^{-1}$]**	**Discrete**	**0.72**	**(0.27, 0.29, 0.33, 0.37, 0.42, 0.48, 0.58, 0.72)**
X5	**External Window**	**(U, SHGC) [$Wm^{-2}K^{-1}$, -]**	**Discrete**	**(2.80, 0.75)**	**(1.71,0.67), (1.80,0.33), (2.80,0.75)**
X6					
X7	WWR - East (E)	--	--	0.15	0.15 (constant)
X8	WWR - West (W)	--	--	0.15	0.15 (constant)
X9	**WWR - South (S)**	--	**Continuous uniform**	**0.30**	**[0.30, 0.50]**
X10	**WWR - North (N)**	--	**Continuous uniform**	**0.20**	**[0.20, 0.40]**
X11	Shading - East (E)	$SC_{Shading}$	--	0	0 (constant)
X12	Shading - West (W)	$SC_{Shading}$	--	0	0 (constant)
X13	**Shading - South (S)**	**$SC_{Shading}$**	**Discrete**	**0**	**(0.4, 1.0)**
X14	Shading - North (N)	$SC_{Shading}$	--	0	0 (constant)

Table 12: Structures of typical external windows

No.	Structure	U-value [$Wm^{-2}K^{-1}$]	SHGC [-]
1 (Base)	**Double-layer Glass（6 +12A+6）**	**2.80**	**0.75**
2	Triple-layer Glass（6 +12A+6 +12A+6）	1.71	0.67
3	Double-layer Low-E Glass（6 Low-E+12A+6）	1.80	0.33

3.4 Analysis of the Pareto-front solution set for typical cities

After selection and evolution from generation to generation, the initial solutions gradually approached the three goals and finally formed an optimal solution set curve named the Pareto-front solution set. Taking Wuhan as an example to analyze the final three-dimensional Pareto-front solution set, the conflict between the three objectives is shown in Figure 10. The red dots in the top figure represent the Pareto-front solution set, and the three figures below represent the projection of this three-dimensional figure onto different planes. In Figure 10a the relationship between LCC and TDR are mutually restricted, and the solution with lower TDR is accompanied by higher LCC. In Figure 10b, LCC and EUI are mutually restricted, the solution with higher LCC consumes less energy, and the solution with lower LCC consumes more energy.

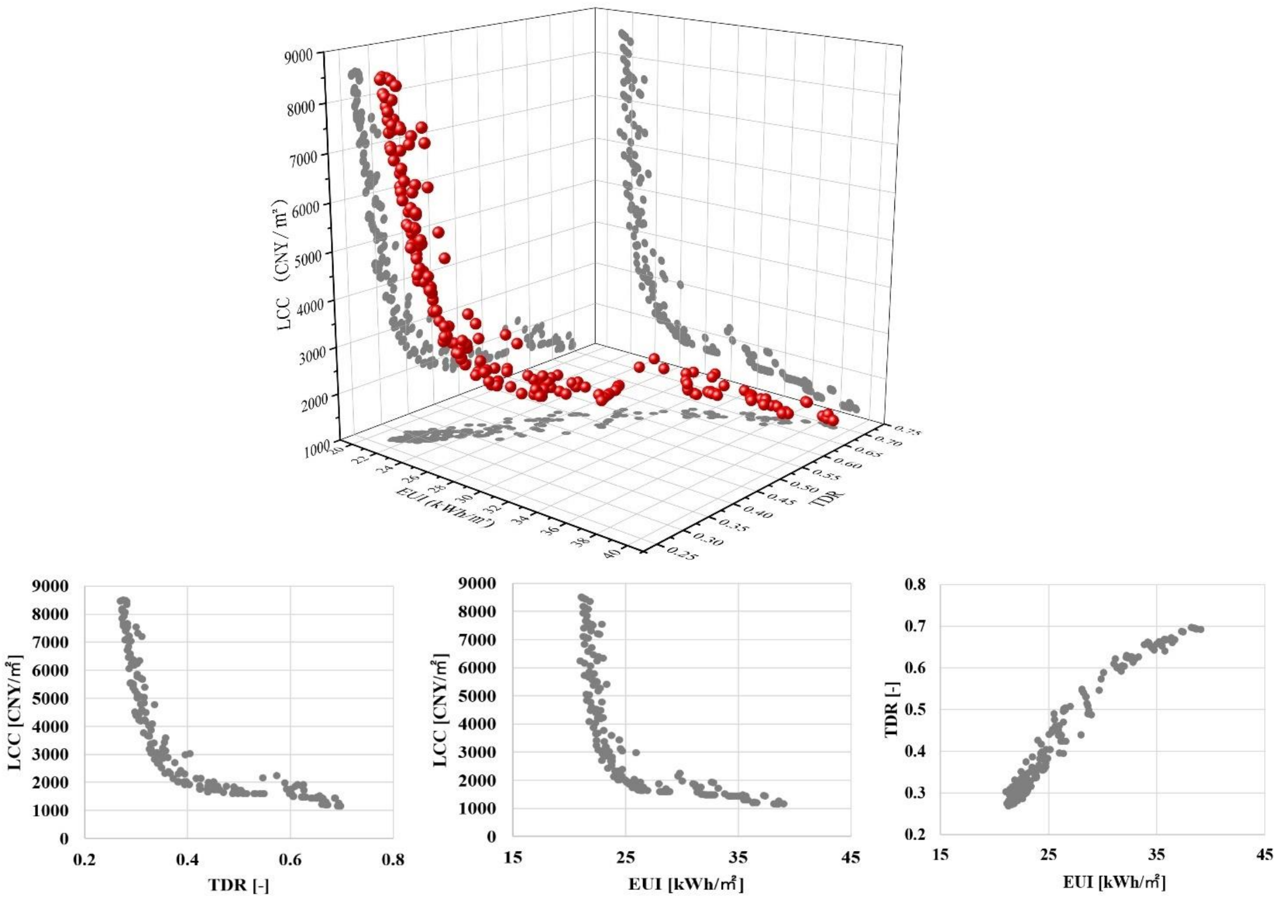

(a) Relationship between LCC and TDR (b) Relationship between LCC and EUI (c) Relationship between TDR and EUI

Figure 10: Scenarios analysis of the Pareto-front solution set (Wuhan)

The analysis of two-dimensional Pareto-front solution set for other seven typical cities can be seen in Figure 11. In all typical cities, the relationship between LCC and TDR are mutually restricted, while the relationship between LCC and EUI are also mutually restricted. Due to the complex relationship between the three objectives, it is not possible to directly judge the optimal solution that meets the three objectives of low energy consumption, low cost and low thermal discomfort hours. More analysis and trade-offs between the three objectives are necessary to work out the best solution among candidates within the Pareto-front solution set.

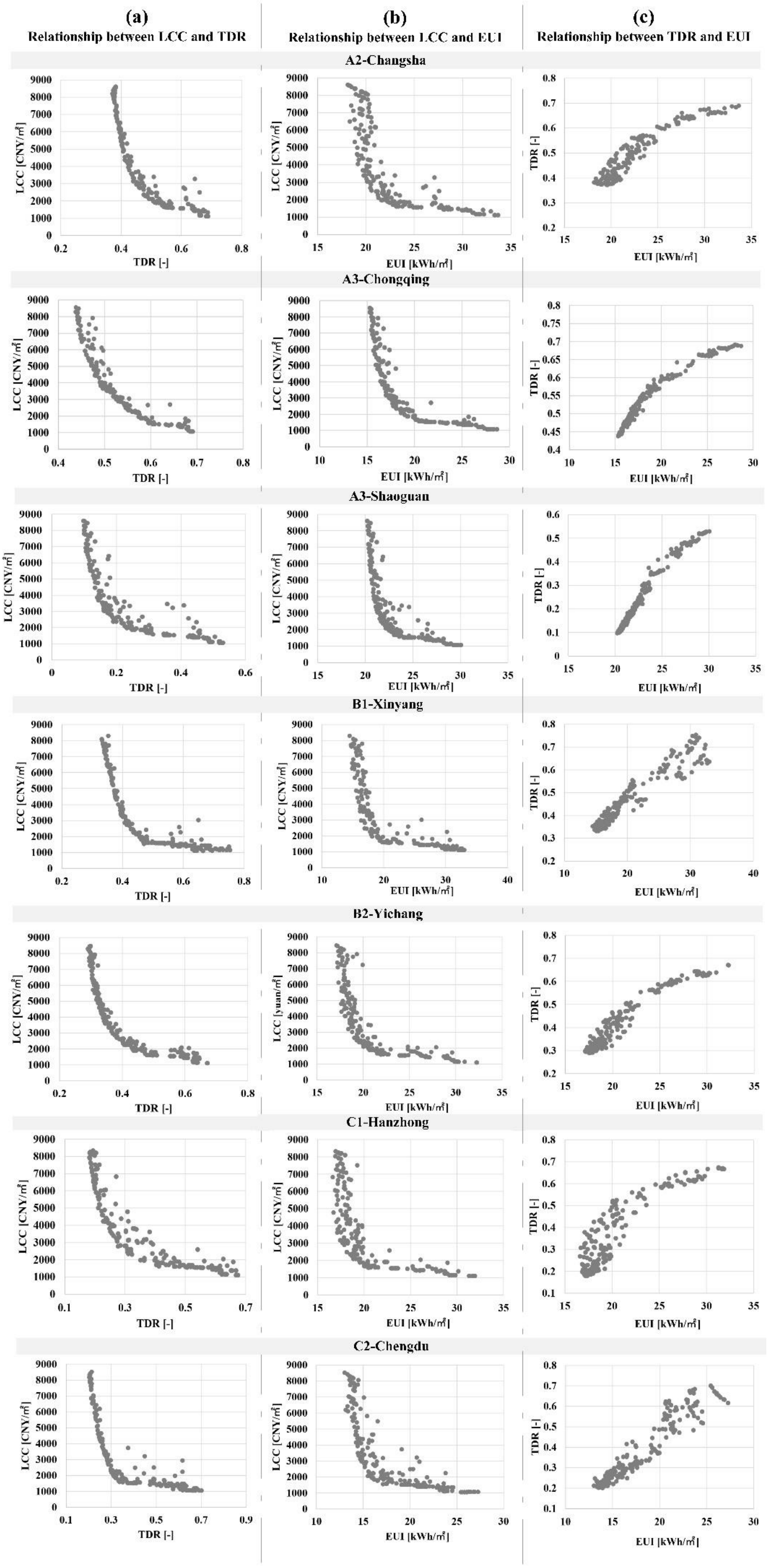
(a)
Relationship between LCC and TDR
(b)
Relationship between LCC and EUI
(c)
Relationship between TDR and EUI
A2-Changsha
A3-Chongqing
A3-Shaoguan
B1-Xinyang
B2-Yichang
C1-Hanzhong
C2-Chengdu
LCC [CNY/m²]
LCC [yuan/m²]
TDR [-]
EUI [kWh/m²]

Figure 11: Analysis of two-dimensional Pareto-front solution set for other seven typical cities

3.5 Analysis of the integrated optimal solution in typical cities

Using the TOPSIS decision-making method, the three-dimensional Euclidean distance of each solution in each city was calculated. Matrix V was obtained by normalizing and weighting the Pareto-front solution set, the Euclidean distance D^{+} and D^{-} of each solution was calculated, and their relative closeness to the ideal solution C^{*} for each solution was obtained. All solutions in the Pareto-front set are ranked according to the values of C^{*}. The point with the maximum value of C^{*} was determined to be the best solution (Figure 12). More detailed information about the calculated results for the top twenty solutions in Wuhan can be found in Table 13.

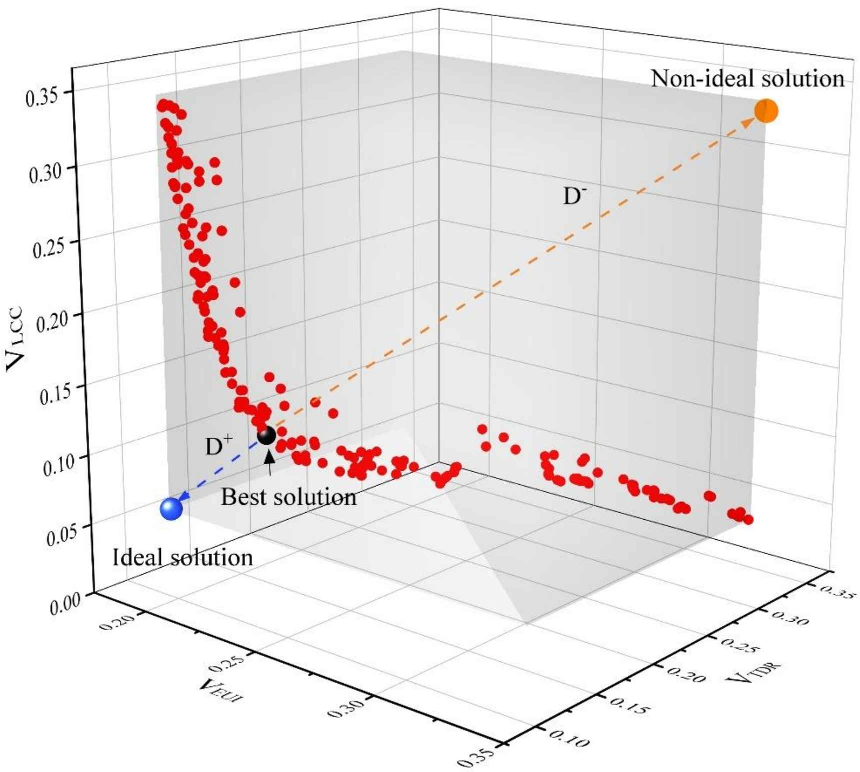

Figure 12: Best solution obtained by using TOPSIS on the Wuhan Pareto-front set

Table 13: Information about the top twenty solutions in Wuhan

Rank	Objectives Matrix [D]			Normalized matrix [R]			Weighted matrix [V]			3D Euclidean distance		
	C_1-EUI $[kWh \cdot m^{-2}]$	C_2-TDR [-]	C_3-LCC [CNY$\cdot m^{-2}$]	Ra	Rb	Rc	Va	Vb	Vc	D^{+}	D^{-}	C*
1	23.80	0.35	2519.34	0.6094	0.5013	0.2965	0.2031	0.1671	0.0988	0.0699	0.3156	0.8187
2	23.78	0.35	2519.49	0.6089	0.5019	0.2965	0.2030	0.1673	0.0988	0.0699	0.3155	0.8185
3	24.87	0.38	2012.17	0.6367	0.5497	0.2368	0.2122	0.1832	0.0789	0.0718	0.3192	0.8163
4	24.73	0.36	2379.87	0.6330	0.5208	0.2801	0.2110	0.1736	0.0934	0.0728	0.3132	0.8113
5	23.82	0.34	2675.60	0.6099	0.4898	0.3149	0.2033	0.1633	0.1050	0.0729	0.3130	0.8112

6	24.49	0.39	2008.50	0.6271	0.5641	0.2364	0.2090	0.1880	0.0788	0.0741	0.3184	0.8111
7	23.71	0.35	2678.05	0.6071	0.4948	0.3152	0.2024	0.1649	0.1051	0.0734	0.3124	0.8097
8	24.35	0.40	2007.80	0.6235	0.5715	0.2363	0.2078	0.1905	0.0788	0.0756	0.3177	0.8077
9	24.14	0.38	2295.72	0.6180	0.5482	0.2702	0.2060	0.1827	0.0901	0.0749	0.3132	0.8070
10	23.69	0.34	2821.64	0.6065	0.4825	0.3321	0.2022	0.1608	0.1107	0.0762	0.3107	0.8030
11	23.84	0.34	2813.99	0.6104	0.4836	0.3312	0.2035	0.1612	0.1104	0.0765	0.3102	0.8021
12	23.46	0.39	2416.66	0.6006	0.5547	0.2844	0.2002	0.1849	0.0948	0.0776	0.3109	0.8003
13	25.12	0.40	1921.34	0.6430	0.5795	0.2261	0.2143	0.1932	0.0754	0.0791	0.3168	0.8003
14	26.34	0.40	1920.83	0.6743	0.5659	0.2260	0.2248	0.1886	0.0753	0.0808	0.3151	0.7960
15	24.25	0.40	2292.83	0.6208	0.5665	0.2698	0.2069	0.1888	0.0899	0.0796	0.3100	0.7956
16	22.97	0.33	3032.83	0.5881	0.4721	0.3569	0.1960	0.1574	0.1190	0.0807	0.3095	0.7932
17	23.34	0.35	2853.27	0.5975	0.5060	0.3358	0.1992	0.1687	0.1119	0.0801	0.3068	0.7931
18	22.97	0.35	2936.43	0.5881	0.4957	0.3456	0.1960	0.1652	0.1152	0.0805	0.3077	0.7927
19	22.90	0.38	2701.99	0.5864	0.5385	0.3180	0.1955	0.1795	0.1060	0.0806	0.3072	0.7921
20	23.08	0.35	2931.18	0.5910	0.4987	0.3449	0.1970	0.1662	0.1150	0.0810	0.3069	0.7913

With the multi-objective model and multi-criteria decision-making process, the top solution shown in Table 13 was selected as a final optimal passive solution for Wuhan, in which the U-values of the external wall and roof are 0.53 $Wm^{-2}K^{-1}$ and 0.48 $Wm^{-2}K^{-1}$, respectively. The recommended external window type is triple-layer glass with a U-value of 1.71$Wm^{-2}K^{-1}$ and an SHGC of 0.67. As illustrated in Figure 13, with all the passive technologies, the annual EUI for heating and cooling could be reduced to 23.80$kWh \cdot m^{-2}$, achieving an EUI saving of 39.6% compared with the base case model through passive optimization. Meanwhile with the EER and COP of HVAC equipment should be improved to no less than 3.30 and 2.80, respectively, the energy consumption could be controlled to within 20 $kWh \cdot m^{-2}$.

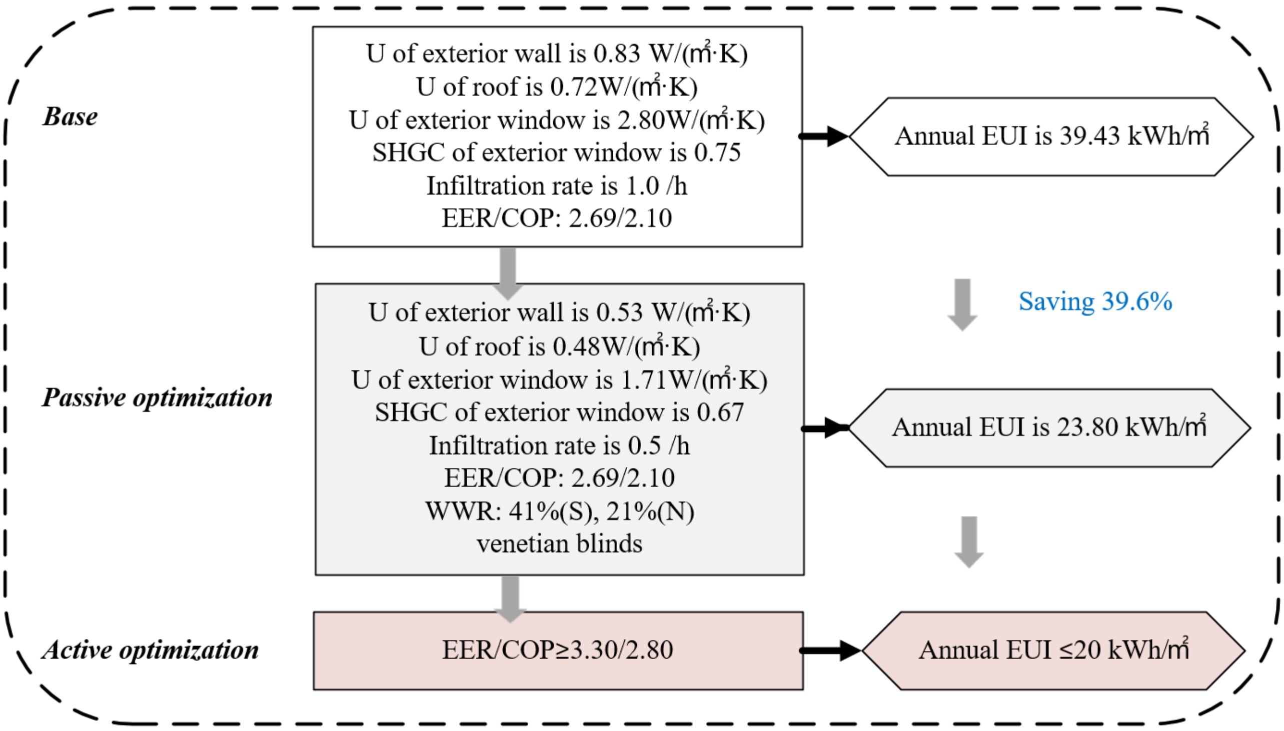

Figure 13: Integrated solution based on energy consumption quota, Wuhan

Table 14 shows the integrated optimal solution that ranks first in each typical city, including the recommended U-value of the envelope, external window types, shading types, and the EER and COP of HVAC equipment. For all typical cities, the recommended U-values of external walls range from 0.53 to 0.65 $Wm^{-2}K^{-1}$, the U-value of roofs range from 0.42 to 0.58 $Wm^{-2}K^{-1}$. Triple-layer glass is recommended in buildings in Area I and Area II, and Low-E glass is recommended in buildings in Area III. The south WWR ranges from 32% to 45%, while the north WWR ranges from 20% to 25%. The infiltration rates are all $0.5h^{-1}$. Venetian blinds are recommended in all solutions. To reach the target EUI, the recommended EER for cooling ranges from 2.69 to 3.30, and the recommended COP for heating ranges from 2.10 to 2.80.

Table 14: Integrated optimal solutions of typical cities in the HSCW zone

Area	**Cities**	**Passive optimal solution**							**EER/COP of HP**
		U of external wall [$Wm^{-2}K^{-1}$]	**U of roof** [$Wm^{-2}K^{-1}$]	**External window (U, SHGC)** [$Wm^{-2}K^{-1}$, --]	**WWR (South)**	**WWR (North)**	**Shading types**	**Infiltration rate** [h^{-1}]	
I	Hanzhong	0.53	0.42	(1.71, 0.67)	45%	25%	Venetian blinds	0.5	＞2.69/2.10
	Chengdu	0.53	0.42	(1.71, 0.67)	39%	24%	Venetian blinds	0.5	＞2.69/2.10
II	Wuhan	0.53	0.48	(1.71, 0.67)	41%	21%	Venetian blinds	0.5	＞3.30/2.80
	Changsha	0.53	0.48	(1.71, 0.67)	34%	20%	Venetian blinds	0.5	＞3.10/2.50
	Xinyang	0.53	0.48	(1.71, 0.67)	45%	23%	Venetian blinds	0.5	＞2.69/2.10
	Yichang	0.53	0.48	(1.71, 0.67)	45%	21%	Venetian blinds	0.5	＞3.10/2.50
III	Chongqing	0.65	0.58	(1.80, 0.33)	36%	20%	Venetian blinds	0.5	＞3.10/2.50
	Shaoguan	0.65	0.58	(1.80, 0.33)	32%	20%	Venetian blinds	0.5	＞3.20/2.70

4. Discussion

4.1 Technical principles for residential buildings in the HSCW zone

According to the results of the integrated optimal solution for residential buildings in eight typical cities, the strategic and technical solutions for reducing energy consumption and improving indoor comfort in this region can be summarized in the following three principles:

1) The proper thermal insulation performance of the envelope

The function of the building envelope is to block outdoor heat from entering the room in summer and reduce heat transfer from indoors to outdoors in winter. Hence, it is necessary to improve the thermal insulation performance of the envelope. However, there may be an overheating risk for well-insulated residential buildings in summer, especially in hot summer regions [68-71], and an excessively insulated envelope is not preferred owing to its higher initial investment, which remains a primary barrier to property developers [72].

Therefore, this study considered trade-offs between the multi-objectives of investment, comfort and energy consumption, and worked out the proper U values for the envelope of residential buildings in the HSCW zone. Since the cooling and heating demand for each city is different, the optimal U-value of the envelope and the recommended HVAC equipment efficiency are different. As illustrated in Table 6, Wuhan has the highest demand for both cooling and heating. The recommended U-values of external walls and the roof are 0.53 $Wm^{-2}K^{-1}$ and 0.48 $Wm^{-2}K^{-1}$, respectively. However, the EER and COP of HVAC equipment should be much higher in order to reach the target EUI quota. Both the heating and cooling demand in Changsha, Xinyang and Yichang are relatively high, therefore, the recommended U-values of the envelope in these cities are the same as those of Wuhan, but the recommended values of EER/COP of HVAC equipment are different. Hanzhong and Chengdu are heating-dominated cities with the lowest recommend comprehensive U-value for the envelope. Chongqing and Shaoguan are cooling-dominated cities where the recommended comprehensive U-value of the envelope is the highest.

2) Variable SHGC design of external windows

External windows are also a key element of the envelope and have a great impact on building energy consumption. The $SHGC_{com}$ of an external window represents the fraction of solar radiation penetrating through a window, including the heat transmitted and absorbed. In summer, windows with a low $SHGC_{com}$ value significantly reduce the cooling load by blocking solar heat from entering the house; while in winter, a high $SHGC_{com}$ value is expected to maximize solar heat gain. Therefore, a balance should be achieved between the cooling load in summer and heating load in winter. Several studies [53, 73] concluded that seasonally adaptable shading can contribute to a variable SHGC value for a window, which is the best compromise for annual heating and cooling demand.

This study worked out the variable SHGC value of external window in different cities in the HSCW zone. The most energy-efficient window type among the three candidates in most cities is the triple-layer glass. The U-value and SHGC of the triple-layer glass are 1.71 $Wm^{-2}K^{-1}$ and 0.67, respectively. The $SHGC_{com}$ of the external window involves the solar heat gain coefficient of the window and shading devices, and can be calculated by $SHGC_{com} = SHGC_{win} \times SC_{shading}$ [63]. All the buildings in typical cities should apply external Venetian blinds. Therefore, the optimal value of the solar heat gain coefficient of the external window, $SHGC_{com}$, is variable. In winter, no external shading devices are applied, the $SHGC_{com}$ of an external window is 0.67, which allows the majority of the solar radiation to enter the room and can reduce the heating load. In summer, external shading devices are applied, and the $SHGC_{com}$ of an external window is 0.27 with the shading devices, which reduces the influence of solar radiation so as to reduce the cooling load. The values of $SHGC_{com}$ of an external window could be 0.27 in summer and 0.67 in winter. It is worth noticing that for completely cooling-dominated cities, such as

Shaoguan and Chongqing (Table 14), triple glass is not recommended due to the relatively low energy saving and high cost. In such cities, double Low-E glass is more cost-effective.

3) Airtightness and indoor air quality

The sensitivity study in section 3.3 found infiltration rate to be the most important passive design factor affecting the annual heating and cooling load in the HSCW zone, and that finding is confirmed by other research [35]. The improvement of airtightness means fresh air infiltration through the doors and windows is reduced. When the airtightness level is too high, mechanical ventilation systems are necessary to provide fresh air for residents' health, which will increase the energy consumption by requiring a fan. Therefore, consideration is needed to determine the airtightness level and ventilation mode of the building.

In this study, the recommended values of the infiltration rate for all typical cities are $0.5h^{-1}$. This meets the minimum requirement of fresh air for residents in residential buildings [74]. In other words, for this level of airtightness, the fresh air that penetrates into the room when the doors and windows are closed can meet the minimum requirement of fresh air for occupants, and no additional mechanical fresh air systems are needed. Therefore, natural ventilation mode is preferred in all cities.

4.2 Recommend solutions for residential buildings in the HSCW zone

Through analysis of the recommended solutions for the typical cities discussed in Section 3.5, this section summarizes the recommended solutions based on the EUI quota for residential buildings in the whole HSCW zone. Reginal policymakers commonly prefer slightly less fined division for the sake of avoiding the complexity of implementation in reality. Based on this request, the recommended solutions for the whole HSCW zone can be clustered into three categories: Area I, Area II and Area III. The recommended solutions in three areas are described in Figure 14. The finer division of seven zones forms solid evidence for individual cities in developing local technical guidance of building design.

Area I, marked blue in Figure 14, coves sub-climatic zones C1 and C2 proposed by Xiong [60]. Area I stands for the cold area, which is a heating-dominated area that includes Hanzhong, Chengdu and other cities in the west of the HSCW zone. For relatively heating-dominated areas, a lower U-value for the envelope can help reduce the heating load; the U-values of the external walls and roof are 0.53 $Wm^{-2}K^{-1}$ and 0.42 $Wm^{-2}K^{-1}$, respectively. Triple-layer glass with movable shading devices are recommended in this area, the U-value of an external window is $1.71Wm^{-2}K^{-1}$, while the values of $SHGC_{com}$ are 0.67 on normal days and 0.27 in summer. The climate of this area is relatively moderate and annual total heating and cooling demand is low, therefore the EER and COP of HVAC equipment are the lowest. This means an HP with lower efficiency can be applied in this area.

Area II, marked orange in Figure 14, coves sub-climatic zones A1, A2, B1 and B2 proposed by Xiong [60]. Area II stands for the area where both heating and cooling demand are high, which means the technologies applied should balance between the impact on both heating and cooling load. Lower U-values of the external walls and roofs are recommended in this area. Variable values for the SHGC of an external window are more important in this area to balance the heating and cooling load. Triple-layer glass and movable shading devices are also recommended in this area. Since the total heating and cooling demand is high, in addition to conventional shading devices, the application of more variable technologies is encouraged, such as night ventilation. It has proved to be an effective way to reduce the cooling load in Shanghai, which is located in Area II [75]. For the performance of an HP, the EER should be no less than 3.30 and the COP should be no less than 2.80, which means the HP with the highest energy efficiency should be used in this area

Area III, marked red in Figure 14, coves sub-climatic zones A3 proposed by Xiong [60]. Area III stands for the hot area, which is a cooling-dominated area including Chongqing, Shaoguan and other cities located in the southwest and south part of the HSCW zone. The SHGC of an external window is one of the most important energy-saving factors in cooling-dominated areas [35, 76]. Double Low-E glass reaches a better energy balance between annual heating and cooling load than triple-layer glass in this area. Therefore, the lowest value of $SHGC_{com}$ is recommended for an external window in this area, which is 0.33 on normal days and can be much lower when shading devices are applied in summer. For cooling-dominated areas, the application of some other unconventional technologies is encouraged to reduce solar heat gain. These include reflective coatings [77-79] and green or cool roofs [80-82], which are proven to successfully reduce the cooling load cost-effectively in a hot summer area. In addition, to reach the energy quota target, the EER should be no less than 3.20 and the COP should be no less than 2.70.

As shown in Figure 14, a natural ventilation mode is preferred in all cities and the recommended value for the infiltration rate for all typical cities is $0.5h^{-1}$.

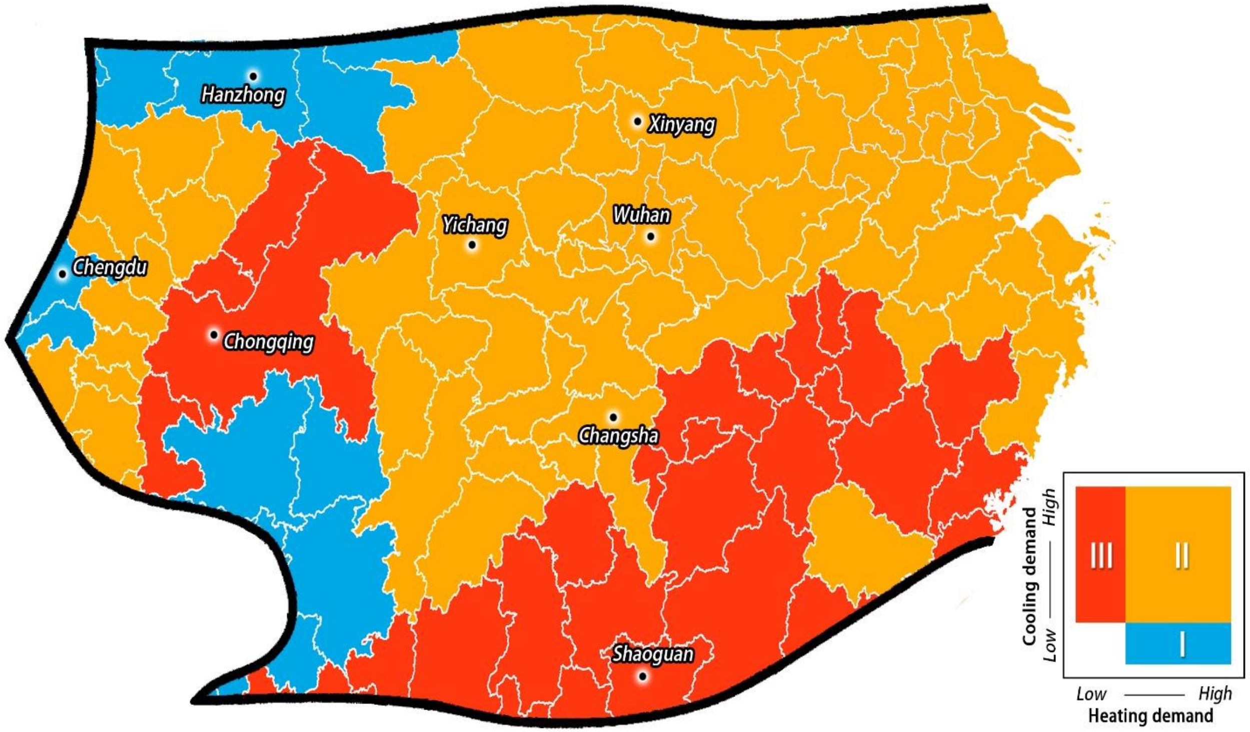

Area I:

（Sub-climatic zones C1&C2）

- ***Heating dominate*** area.
- Annual total heating and cooling demand is the lowest.

Area II:

（Sub-climatic zones A1&A2&B1&B2）

- Both ***heating and cooling*** demand are high.
- Annual total heating and cooling demand is the highest.

Area III:

（Sub-climatic zones A3）

- ***Cooling dominate*** area.
- Annual total heating and cooling demand is the medium.

Recommended Solutions

Area	Cities	U of External wall $[Wm^{-2}K^{-1}]$	U of Roof $[Wm^{-2}K^{-1}]$	External window		WWR		Infiltration rate $[h^{-1}]$	Shading	EER/COP of HP	Notes
				Type	(U, SHGC) $[Wm^{-2}K^{-1}, -]$	South	North				
I	Hanzhong Chengdu	≤0.53	≤0.42	Triple glass	(1.71, 0.67)	≤45%	≤30%	0.5	Venetian blinds	≥2.69/2.10	➢ Natural ventilation
II	Wuhan Xinyang Changsha Yichang	≤0.53	≤0.48	Triple glass	(1.71, 0.67)	≤45%	≤30%	0.5	Venetian blinds	≥3.30/2.80	➢ Natural ventilation ➢ Night ventilation is encouraged to be applied.
III	Chongqing Shaoguan	≤0.65	≤0.58	Double Low-E glass	(1.80, 0.33)	≤40%	≤30%	0.5	Venetian blinds	≥3.20/2.70	➢ Natural ventilation ➢ Reflective coatings and cool roofs are encouraged to be applied.

Figure 14: The recommended solutions for residential buildings in the whole HSCW zone

5. Conclusions

In the light of the implementation of the government's energy consumption quota policies, this paper presents a novel three-step model that consists of three processes: (1) multi-objective optimization, (2) multi-criteria decision-making and (3) integrated solutions analysis. By applying this model, this paper proposes strategic and technical solutions for residential buildings in the whole HSCW zone for the first time. The proposed optimal integrated solutions are composed of both passive and active measures to improve building thermal performance, to reduce the burden on artificial heating and cooling while improving the performance of air conditioning in extreme weather conditions. The three-step optimization approach and solutions proposed here fill the knowledge gaps that are lacking in the integrated technical guidance for residential buildings based on the EUI quota in this region. The main results and findings of this study are as follows:

1) A base building combining a typical architectural layout with a typical local resident's energy use behaviour was set up. The passive design factors with an important influence on the annual total heating and cooling load were identified. The top seven factors were: infiltration rate, the U value of external walls, the SHGC of external windows, south shading type, south window-to-wall ratio, north window-to-wall ratio and the U value of the roof.
2) A novel three-step, multi-objective, optimization model targeting the EUI quota was developed. The model not only includes the conventional optimization process using the NSGA-II optimization algorithm but also considers a post-optimization process to trade-off among the three objectives of energy, comfort and economy to determine the best passive design solution for residential buildings. Besides, it was found that the optimal integrated solutions can be worked out through the model.
3) This study mapped the full spectrum of solutions and provides rigorous evidence to energy policymakers for forthcoming design standards. (1) For relatively heating-dominated areas located in the northwest part of the HSCW zone, a lower U-value of the envelope, variable $SHGC_{com}$ for external windows with shading devices, and the lowest EER/COP of HP is recommended in order to reach the energy quota target. (2) For areas where both heating and cooling demand are high, located in the middle-east of the HSCW zone, the use of a heat pump with the highest EER/COP is recommended. (3) For relatively cooling-dominated areas located in the south part of the HSCW zone, the lowest value of SHGC for external windows is recommended, and the application of some other unconventional technologies, such as reflective coatings and green or cool roofs, is encouraged.

4) The research outcomes lie a foundation for building thermal design regulation in the hot summer and cold winter zone which provides rigorous evidence for policy-makers.

Acknowledgement

The research is jointly sponsored by the 13th Five-Year Plan National Key R&D Programme "Solutions to Heating and Cooling of Buildings in the Yangtze River Region (SSHCool)" [Grant No: 2016YFC0700301] in association with the UK-China collaborative research project "Low carbon climate-responsive Heating and Cooling of Cities (LoHCool)" funded by the Natural Science Foundation of China [NSFC Grant No. 51561135002] and the UK Engineering and Physical Sciences Research Council [EPSRC Grant No. EP/N009797/1]. This research is also supported by the Innovation Research Project Funds for Graduates in Chongqing, China [Grant No. CYB15040]. Cao Xinyun would like to thank China Scholarship Council for the sponsorship for her one-year academic visit to Lawrence Berkeley National Laboratory in the US (Grant No.201806050242). The authors would like to thank Mr Kaixuan Wang and Miss Zhaoyang Chen for their assistance with the operation of the software programme.

References

[1] IPCC, Climate Change 2014: Synthesis Report, in: Contribution of Working Groups I, II and III to the Fifth Assessment Report of the Intergovernmental Panel on Climate Change, IPCC, Geneva, Switzerland, 2014.

[2] IEA, Key World Energy Statistics 2019, in, 2019.

[3] H. Duan, J. Mo, Y. Fan, S. Wang, Achieving China's energy and climate policy targets in 2030 under multiple uncertainties, Energy Economics, 70 (2018) 45-60.

[4] N. Zhou, N. Khanna, W. Feng, J. Ke, M. Levine, Scenarios of energy efficiency and CO2 emissions reduction potential in the buildings sector in China to year 2050, Nature Energy, (2018).

[5] B. Li, C. Du, R. Yao, W. Yu, V. Costanzo, Indoor thermal environments in Chinese residential buildings responding to the diversity of climates, Applied Thermal Engineering, 129 (2018).

[6] A.-P.E. Cooperation, APEC Energy Demand and Supply Outlook 6th Edition, in, Asia Pacific Energy Research Center (APERC), Japan, 2016.

[7] C. Peng, Y. Jiang, Roadmap for China's Building Energy Conservation (in Chinese), China Architecture & Building Press, Beijing, 2015.

[8] B. Li, R. Yao, Building energy efficiency for sustainable development in China: challenges and opportunities, Building Research & Information, 40 (4) (2012) 417-431.

[9] J. Li, B. Shui, A comprehensive analysis of building energy efficiency policies in China: status quo and development perspective, Journal of Cleaner Production, 90 (2015) 326-344.

[10] Q. Hu, X. Li, A. Lin, W. Qi, X. Li, X.J. Yang, Total emission control policy in China, Environmental Development, 25 (2018) 126-129.

[11] W. Feng, Q. Zhang, H. Ji, R. Wang, N. Zhou, Q. Ye, B. Hao, Y. Li, D. Luo, S.S.Y. Lau, A review of net zero energy buildings in hot and humid climates: Experience learned from 34 case study buildings, Renewable and Sustainable Energy Reviews, 114 (2019) 109303.

[12] Z. Liu, Q. Zhou, Z. Tian, B.-j. He, G. Jin, A comprehensive analysis on definitions, development, and policies of nearly zero energy buildings in China, Renewable and Sustainable Energy Reviews, 114 (2019) 109314.

[13] X. Li, R. Yao, Q. Li, Y. Ding, B. Li, An object-oriented energy benchmark for the evaluation of the office building stock, Utilities Policy, 51 (2018) 1-11.

[14] C. The State Council, Work plan for controlling greenhouse gas emissions during the 13th five-year plan period, in: C. The State Council (Ed.), http://www.gov.cn/zhengce/content/2016-11/04/content_5128619.htm (Accessed date: May 17, 2020).

[15] Y. Jiang, C. Peng, D. Yan, Roadmap for China's Building Energy Conservation (in Chinese), Construction Science and Technology, (17) (2012) 12-19.

[16] MOST, 2016 national project R & D program key project application guidelines, in, http://www.most.gov.cn/mostinfo/xinxifenlei/fgzc/gfxwj/gfxwj2016/201602/t20160222_124196.htm (Accessed date: May 15, 2020).

[17] R. Yao, V. Costanzo, X. Li, Q. Zhang, B. Li, The effect of passive measures on thermal comfort and energy conservation. A case study of the hot summer and cold winter climate in the Yangtze River region, Journal of Building Engineering, 15 (2018) 298-310.

[18] G. Zhang, X. Li, W. Shi, B. Wang, Z. Li, Y. Cao, Simulations of the energy performance of variable refrigerant flow system in representative operation modes for residential buildings in the hot summer and cold winter region in China, Energy and Buildings, 174 (2018) 414-427.

[19] Z. Wang, R. de Dear, B. Lin, Y. Zhu, Q. Ouyang, Rational selection of heating temperature set points for China's hot summer - Cold winter climatic region, Building and Environment, 93 (2015) 63-70.

[20] C.A. Short, J. Song, L. Mottet, S. Chen, J. Wu, J. Ge, Challenges in the low-carbon adaptation of China’s apartment towers, Building Research & Information, 46 (8) (2018) 899-930.

[21] B. Li, R. Yao, Q. Wang, Y. Pan, An introduction to the Chinese Evaluation Standard for the indoor thermal

environment, Energy and Buildings, 82 (2014) 27-36.

[22] N.B.o.S.o. China, China's Statistics Almanac (in Chinese), China Statistics Press, 2019.

[23] H. Jiang, R. Yao, S. Han, C. Du, W. Yu, S. Chen, B. Li, H. Yu, N. Li, J. Peng, B. Li, How do urban residents use energy for winter heating at home? A large-scale survey in the hot summer and cold winter climate zone in the Yangtze River region, Energy and Buildings, 223 (2020) 110131.

[24] F.R. Xiaoqian Qian, Kuangliang Qian, Cong Wang, Energy saving effect of external thermal insulation of residential building under actual energy usage condition in hot summer and cold winter zone (in Chinese), HVAC Journal, 07 (2017) 46-50.

[25] N. Li, Q. Chen, Experimental study on heat transfer characteristics of interior walls under partial-space heating mode in hot summer and cold winter zone in China, Applied Thermal Engineering, 162 (2019) 114264.

[26] J. Yu, C. Yang, L. Tian, D. Liao, A study on optimum insulation thicknesses of external walls in hot summer and cold winter zone of China, Applied Energy, 86 (11) (2009) 2520-2529.

[27] L. Derradji, K. Imessad, M. Amara, F. Boudali Errebai, A study on residential energy requirement and the effect of the glazing on the optimum insulation thickness, Applied Thermal Engineering, 112 (2017) 975-985.

[28] D. O'Connor, J.K.S. Calautit, B.R. Hughes, A review of heat recovery technology for passive ventilation applications, Renewable and Sustainable Energy Reviews, 54 (2016) 1481-1493.

[29] G. Cao, H. Awbi, R. Yao, Y. Fan, K. Sirén, R. Kosonen, J. Zhang, A review of the performance of different ventilation and airflow distribution systems in buildings, Building and Environment, 73 (2014) 171-186.

[30] H.-Y. Chan, S.B. Riffat, J. Zhu, Review of passive solar heating and cooling technologies, Renewable and Sustainable Energy Reviews, 14 (2) (2010) 781-789.

[31] M. Konstantoglou, A. Tsangrassoulis, Dynamic operation of daylighting and shading systems: A literature review, Renewable and Sustainable Energy Reviews, 60 (2016) 268-283.

[32] B. Si, Z. Tian, X. Jin, X. Zhou, X. Shi, Ineffectiveness of optimization algorithms in building energy optimization and possible causes, Renewable Energy, 134 (2019) 1295-1306.

[33] H. Li, S. Wang, Coordinated optimal design of zero/low energy buildings and their energy systems based on multi-stage design optimization, Energy, 189 (2019) 116202.

[34] F. Ascione, N. Bianco, G. Maria Mauro, D.F. Napolitano, Building envelope design: Multi-objective optimization to minimize energy consumption, global cost and thermal discomfort. Application to different Italian climatic zones, Energy, 174 (2019) 359-374.

[35] S. Gou, V.M. Nik, J.-L. Scartezzini, Q. Zhao, Z. Li, Passive design optimization of newly-built residential buildings in Shanghai for improving indoor thermal comfort while reducing building energy demand, Energy and Buildings, 169 (2018) 484-506.

[36] X. Chen, H. Yang, A multi-stage optimization of passively designed high-rise residential buildings in multiple building operation scenarios, Applied Energy, 206 (2017) 541-557.

[37] Y. Schwartz, R. Raslan, D. Mumovic, Implementing multi objective genetic algorithm for life cycle carbon footprint and life cycle cost minimisation: A building refurbishment case study, Energy, 97 (2016) 58-68.

[38] E. Asadi, M.G.d. Silva, C.H. Antunes, L. Dias, L. Glicksman, Multi-objective optimization for building retrofit: A model using genetic algorithm and artificial neural network and an application, Energy and Buildings, 81 (2014) 444-456.

[39] Y. Bichiou, M. Krarti, Optimization of envelope and HVAC systems selection for residential buildings, Energy and Buildings, 43 (12) (2011) 3373-3382.

[40] R. Jing, M. Wang, Z. Zhang, J. Liu, H. Liang, C. Meng, N. Shah, N. Li, Y. Zhao, Comparative study of posteriori decision-making methods when designing building integrated energy systems with multi-objectives, Energy and Buildings, 194 (2019) 123-139.

[41] K. Deb, A. Pratap, S. Agarwal, T. Meyarivan, A fast and elitist multiobjective genetic algorithm: NSGA-II, IEEE Transactions on Evolutionary Computation, 6(2) (2002) 182-197.

[42] S. Attia, M. Hamdy, W. O'Brien, S. Carlucci, Assessing gaps and needs for integrating building performance optimization tools in net zero energy buildings design, Energy and Buildings, 60 (2013) 110-124.

[43] S. Carlucci, G. Cattarin, F. Causone, L. Pagliano, Multi-objective optimization of a nearly zero-energy building based on thermal and visual discomfort minimization using a non-dominated sorting genetic algorithm (NSGA-II), Energy and Buildings, 104 (2015) 378-394.

[44] F. Harkouss, F. Fardoun, P.H. Biwole, Passive design optimization of low energy buildings in different climates, Energy, 165 (2018) 591-613.

[45] Z. Xu, N. Zhao, Information fusion for intuitionistic fuzzy decision making: An overview, Information Fusion, 28 (2016) 10-23.

[46] E. Wang, N. Alp, J. Shi, C. Wang, X. Zhang, H. Chen, Multi-criteria building energy performance benchmarking through variable clustering based compromise TOPSIS with objective entropy weighting, Energy, 125 (2017) 197-210.

[47] S. Moghtadernejad, L.E. Chouinard, M.S. Mirza, Multi-criteria decision-making methods for preliminary design of sustainable facades, Journal of Building Engineering, 19 (2018) 181-190.

[48] MoHURD, Evaluation standard for indoor thermal environment in civil buildings (GB/T 50785-2012) (in Chinese), in, China Architecture & Building Press, Beijing, China, 2012.

[49] R. Yao, B. Li, J. Liu, A theoretical adaptive model of thermal comfort – Adaptive Predicted MeanVote(aPMV) Building and Environment, 44 (2009) 2089-2096.

[50] W. Long, Design and management of building energy efficiency (in Chinese), China Architecture Publishing & Media Co.,Ltd., 2005.

[51] X. Liu, Y. Chen, H. Ge, P. Fazio, G. Chen, X. Guo, Determination of optimum insulation thickness for building walls with moisture transfer in hot summer and cold winter zone of China, Energy and Buildings, 109 (2015) 361-368.

[52] J.C. Lam, K.K.W. Wan, L. Yang, Sensitivity analysis and energy conservation measures implications, Energy Conversion and Management, 49 (11) (2008) 3170-3177.

[53] S.M. Bambrook, A.B. Sproul, D. Jacob, Design optimisation for a low energy home in Sydney, Energy and Buildings, 43 (7) (2011) 1702-1711.

[54] Y. Cui, Z. Geng, Q. Zhu, Y. Han, Review: Multi-objective optimization methods and application in energy saving, Energy, 125 (2017) 681-704.

[55] F. Kheiri, A review on optimization methods applied in energy-efficient building geometry and envelope design, Renewable and Sustainable Energy Reviews, 92 (2018) 897-920.

[56] P.A. Deb K , Agarwal S , et al., A fast and elitist multiobjective genetic algorithm: NSGA-II, IEEE Transactions on Evolutionary Computation, 6(2) (2002).

[57] N. Delgarm, B. Sajadi, S. Delgarm, Multi-objective optimization of building energy performance and indoor thermal comfort: A new method using artificial bee colony (ABC), Energy and Buildings, 131 (2016) 42-53.

[58] R.A. Krohling, V.C. Campanharo, Fuzzy TOPSIS for group decision making: A case study for accidents with oil spill in the sea, Expert Systems with Applications, 38 (4) (2011) 4190-4197.

[59] E. Wang, Benchmarking whole-building energy performance with multi-criteria technique for order preference by similarity to ideal solution using a selective objective-weighting approach, Applied Energy, 146 (2015) 92-103.

[60] J. Xiong, R. Yao, S. Grimmond, Q. Zhang, B. Li, A hierarchical climatic zoning method for energy efficient building design applied in the region with diverse climate characteristics, Energy and Buildings, 186 (2019) 355-367.

[61] MoHURD, Code for thermal design of civil building, in, China Architecture & Building Press, Beijing, China, 2016.

[62] M. Laetitia, S. Jiyun, S.C. Alan, C. Shuqin, W. Jindong, Y. Wei, X. Jie, Z. Qiulei, G. Jian, L. Meng, Y. Runming, L. Baizhan, The hot summer-cold winter region in China: Challenges in the low carbon adaptation of residential slab buildings to enhance comfort, Energy and Buildings, 223 (2020) 110181.

[63] MoHURD, Design standard for energy efficiency of residential buildings in hot summer and cold winter zone JGJ 134-2010 (in Chinese), in, China Architecture & Building Press, Beijing, China, 2010.

[64] M.D.a.R.C.o. Wuhan, Guide to Energy Consumption Quotas for Civil Buildings in Wuhan (in Chinese), in, Municipal Development and Reform Commission of Wuhan, Wuhan, 2014.

[65] C. Ding, Z. Nan, Using Residential and Office Building Archetypes for Energy Efficiency Building Solutions in an Urban Scale: A China Case Study, Energies, 13 (2020) 3210.

[66] China Residential Energy Consumption Survey, in, Renmin University, Beijing, 2012.

[67] Y. Jiang, Concept Debate for China's Building Energy Conservation (in Chinese), China Architecture & Building Press, Beijing, 2016.

[68] E. Mlecnik, T. Schütze, S.J.T. Jansen, G. de Vries, H.J. Visscher, A. van Hal, End-user experiences in nearly zero-energy houses, Energy and Buildings, 49 (2012) 471-478.

[69] M. Derbez, B. Berthineau, V. Cochet, C. Pignon, J. Ribéron, G. Wyart, C. Mandin, S. Kirchner, A 3-year follow-up of indoor air quality and comfort in two energy-efficient houses, Building and Environment, 82 (2014) 288-299.

[70] R.S. McLeod, C.J. Hopfe, A. Kwan, An investigation into future performance and overheating risks in Passivhaus dwellings, Building and Environment, 70 (2013) 189-209.

[71] K.J. Lomas, T. Kane, Summertime temperatures and thermal comfort in UK homes, Building Research & Information, 41 (3) (2013) 259-280.

[72] S.P. Forrester, T.G. Reames, Understanding the residential energy efficiency financing coverage gap and market potential, Applied Energy, 260 (2020) 114307.

[73] Á.L. León, S. Domínguez, M.A. Campano, C. Ramírez-Balas, Reducing the Energy Demand of Multi-Dwelling Units in a Mediterranean Climate Using Solar Protection Elements, Energies, 5 (9) (2012) 3398-3424.

[74] MoHURD, Code for thermal design of civil buildings GB 51076-2016 (in Chinese), in, China Architecture & Building Press, Beijing, China, 2016.

[75] Z.C. Li, Bin, Night ventilation strategy applied to intermmittent air conditioning buildings in Shanghai (in Chinese), HV & AC, 43 (2013) 73-77.

[76] X. Chen, H. Yang, W. Zhang, Simulation-based approach to optimize passively designed buildings: A case study on a typical architectural form in hot and humid climates, Renewable and Sustainable Energy Reviews, 82 (2018) 1712-1725.

[77] J. Ouyang, C. Wang, H. Li, K. Hokao, A methodology for energy-efficient renovation of existing residential buildings in China and case study, Energy and Buildings, 43 (9) (2011) 2203-2210.

[78] S.M. Porritt, P.C. Cropper, L. Shao, C.I. Goodier, Ranking of interventions to reduce dwelling overheating during heat waves, Energy and Buildings, 55 (2012) 16-27.

[79] M. Pellegrino, M. Simonetti, G. Chiesa, Reducing thermal discomfort and energy consumption of Indian residential buildings: Model validation by in-field measurements and simulation of low-cost interventions, Energy and Buildings, 113 (2016) 145-158.

[80] Y. Gao, J. Xu, S. Yang, X. Tang, Q. Zhou, J. Ge, T. Xu, R. Levinson, Cool roofs in China: Policy review, building simulations, and proof-of-concept experiments, Energy Policy, 74 (2014) 190-214.

[81] Y. Gao, D. Shi, R. Levinson, R. Guo, C. Lin, J. Ge, Thermal performance and energy savings of white and sedum-tray garden roof: A case study in a Chongqing office building, Energy and Buildings, 156 (2017) 343-359.

[82] I. Ziogou, A. Michopoulos, V. Voulgari, T. Zachariadis, Implementation of green roof technology in residential buildings and neighborhoods of Cyprus, Sustainable Cities and Society, 40 (2018) 233-243.